

## Article

# Anti-Proliferative and Cytoprotective Activity of Aryl Carbamate and Aryl Urea Derivatives with Alkyl Groups and Chlorine as Substituents

Maxim Oshchepkov <sup>1,\*</sup>, Leonid Kovalenko <sup>1</sup>, Antonida Kalistratova <sup>1</sup>, Maria Ivanova <sup>1</sup>, Galina Sherstyanykh <sup>2</sup>, Polina Dudina <sup>2</sup>, Alexey Antonov <sup>3</sup>, Anastasia Cherkasova <sup>4</sup> and Mikhail Akimov <sup>2,\*</sup>

<sup>1</sup> Department of Chemistry and Technology of Biomedical Drugs, Mendeleev University of Chemical Technology of Russia, Miusskaya sq. 9, 125047 Moscow, Russia; lkovalenko@muctr.ru (L.K.); kalistratova.a.v@muctr.ru (A.K.); ivanova.ms.rcu@yandex.ru (M.I.)

<sup>2</sup> Shemyakin-Ovchinnikov Institute of Bioorganic Chemistry, Russian Academy of Sciences, Ul. Miklukho-Maklaya, 16/10, 117997 Moscow, Russia; galya24may@gmail.com (G.S.); polinadudkinz@gmail.com (P.D.)

<sup>3</sup> Faculty of Mechanics and Mathematics, Lomonosov Moscow State University, GSP-1, Leninskie Gory, 119991 Moscow, Russia; alexey.p.antonov@gmail.com

<sup>4</sup> Faculty of Biotechnology, Lomonosov Moscow State University, GSP-1, Leninskie Gory, 119991 Moscow, Russia; a-cherkasova2000@mail.ru

\* Correspondence: m.s.oshchepkov@muctr.ru (M.O.); akimovmike@gmail.com (M.A.); Tel.: +7-(495)-330-65-92 (M.A.)



**Citation:** Oshchepkov, M.; Kovalenko, L.; Kalistratova, A.; Ivanova, M.; Sherstyanykh, G.; Dudina, P.; Antonov, A.; Cherkasova, A.; Akimov, M. Anti-Proliferative and Cytoprotective Activity of Aryl Carbamate and Aryl Urea Derivatives with Alkyl Groups and Chlorine as Substituents. *Molecules* **2022**, *27*, 3616. <https://doi.org/10.3390/molecules27113616>

Academic Editor: Baoan Song

Received: 21 April 2022

Accepted: 30 May 2022

Published: 4 June 2022

**Publisher's Note:** MDPI stays neutral with regard to jurisdictional claims in published maps and institutional affiliations.



**Copyright:** © 2022 by the authors. Licensee MDPI, Basel, Switzerland. This article is an open access article distributed under the terms and conditions of the Creative Commons Attribution (CC BY) license (<https://creativecommons.org/licenses/by/4.0/>).

**Abstract:** Natural cytokinins are a promising group of cytoprotective and anti-tumor agents. In this research, we synthesized a set of aryl carbamate, pyridyl urea, and aryl urea cytokinin analogs with alkyl and chlorine substitutions and tested their antiproliferative activity in MDA-MB-231, A-375, and U-87 MG cell lines, and cytoprotective properties in H<sub>2</sub>O<sub>2</sub> and CoCl<sub>2</sub> models. Aryl carbamates with the oxamate moiety were selectively anti-proliferative for the cancer cell lines tested, while the aryl ureas were inactive. In the cytoprotection studies, the same aryl carbamates were able to counteract the CoCl<sub>2</sub> cytotoxicity by 3–8%. The possible molecular targets of the aryl carbamates during the anti-proliferative action were the adenosine A2 receptor and CDK2. The obtained results are promising for the development of novel anti-cancer therapeutics.

**Keywords:** carbamates; oxamates; synthetic cytokinins; substituted ureas; anti-stress effect; cytotoxicity; oxidative stress

## 1. Introduction

The plant hormones cytokinins are predominantly adenine-derived regulatory molecules that take part in almost all stages of plant growth and development. Studies of the biological activity of cytokinins in animal cells, implemented mainly on 6-substituted purines, in particular on kinetin [1,2], have shown the presence of antiviral, antiparasitic, antitumor, antioxidant and other therapeutic properties [3–6]. At the same time, many chemical compounds with cytokinin activity other than substituted purines are known, but their activity has not been investigated on animal and human cells.

One of the promising classes of cytokinin-like compounds are aryl and heteroaryl urea derivatives. Some derivatives, such as 1-phenyl-3-(4-pyridyl) urea (4PU), exhibit surprisingly high cytokinin activity in tobacco callus culture. Some synthetic derivatives were even more active than natural endogenous cytokinins [7,8], but studies of other types of biological activity of these compounds were not carried out. Another class of synthetic cytokinin analogs contain urea and carbamate moieties with an ethylene linker. Among them, the oxalylaryl carbamates (Figure 1, Structure II) have anti-stress growth-regulatory activity for crops [9,10], and ethylene diurea (EDU, Figure 1, III) has ozone protective properties [11–14].

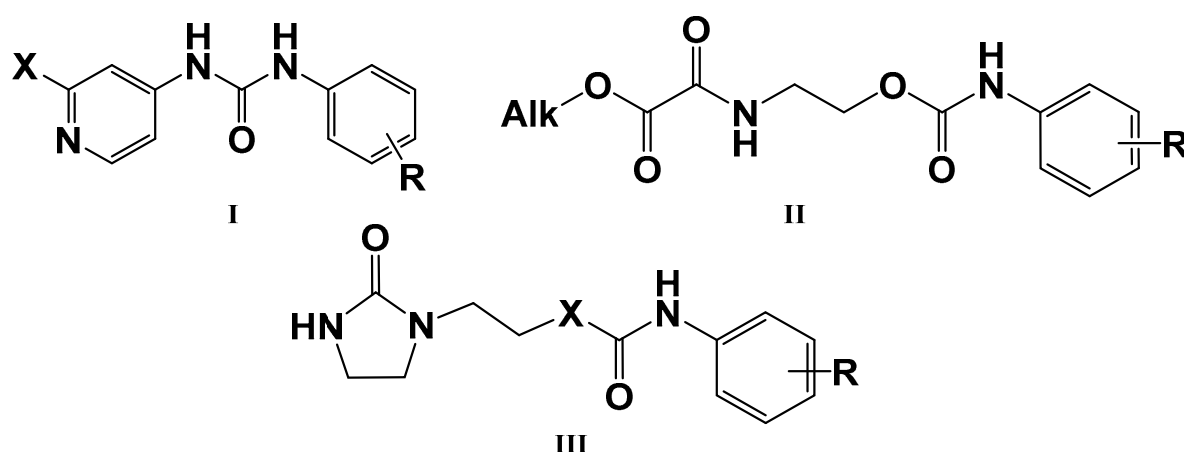


**Figure 1.** Cytokinin-like compounds.

Cytokinin-like phenylureas bind to the same site as cytokinin receptors [15], are stable, resistant to the action of oxidases, and contribute to an increase in the activity of peroxidase and superoxide dismutase.

Chemical modification of cytokinin analogs may result in both an increase in their pro-proliferative effects and in an inversion of their activity. Thus, it was shown that the introduction of substituents into the aromatic ring increases the activity, and electron-withdrawing substituents lead to a greater effect than electron-donating substituents [16]. Chlorine derivatives of nonpurine analogues of cytokinins usually have a higher proliferative activity [17].

In addition to the cytoprotective effect, the analogs of EDU were shown to exhibit anti-cancer activity via ROS-dependent apoptosis induction with  $EC_{50}$  of about 10–20  $\mu$ M [18], but the available data on this topic are quite limited. Earlier we synthesized a series of aryl-substituted ureas and carbamates containing aromatic chlorine and a modified imidazolidinone moiety. These compounds were found to be cytotoxic to the breast cancer cell line MDA-MB-231, glioblastoma U-87 MG and neuroblastoma SH-SY5Y, but not to the melanoma A-375 cell line. The introduction of chlorine into the aromatic ring of cytokinin analogues significantly reduced the cytotoxicity, but at the same time provided the capability to protect cells from oxidative stress induced by  $H_2O_2$  [19]. The observed cytotoxicity was quite low ( $EC_{50}$  of about 100  $\mu$ M) but, given the scarcity of the data, there was a high probability that there could be more active compounds among other similar cytokinin analogs.

In the current research, we tried to find more active analogs of cytokinins with both anti-cancer and cytoprotective activities. We synthesized a novel set of modifications of 4PU (I), EDU (III), and oxalylaryl carbamates (II) with alkyl and chlorine substitutions and evaluated of their anti-proliferative and cytoprotective activity. Aryl carbamates with the oxamate moiety were anti-proliferative for the cancer cell lines tested, while the aryl ureas were inactive. In the cytoprotection studies, all the derivatives displayed little or no activity. The possible molecular targets of aryl carbamates during the anti-proliferative action were the adenosine A2 receptor and CDK2.

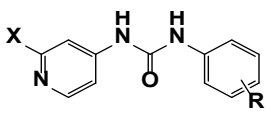
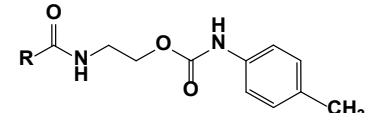
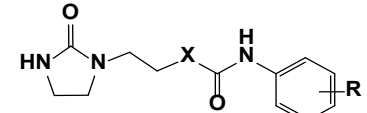
## 2. Results

### 2.1. Compound Synthesis

The preparation of 1-phenyl-3-(4-pyridyl) urea derivatives I (Table 1) was carried out accordingly to known methods [20,21]. The last stage consisted of the interaction of phenyl isocyanate with 4-aminopyridine. To convert 4-aminopyridine and 4-amino-2-chloropyridine salts into the free form and accelerate the process, basic catalysis was used by adding a few drops of triethylamine to the reaction mixture.

Aryl ureas and aryl carbamates (Table 1) were produced by the reaction of corresponding aryl isocyanates with imidazolidinone-substituted alcohol or amine in the presence of triethylamine in anhydrous toluene (for aryl ureas) or acetonitrile (for aryl carbamates) as described in the literature [19]. Oxalylaryl carbamates were obtained in the same way as described in refs. [9,10].

**Table 1.** Structural formulas of synthesized aryl carbamates and ureas.

								
1-Phenyl-3-(4-Pyridyl) Urea Derivatives			Arylcarbamates		Arylureas			
R	X		R		X = O, R		X = NH, R	
Ia	—	H	IIa	iPrO	IIIa	H	IIIe	H
Ib	2-CH <sub>3</sub>	Cl	IIb	nPrOC(O)	IIIb	3-Cl	IIIf	3-Cl
Ic	3-CH <sub>3</sub>	Cl	IIc	iPrOC(O)	IIIc	4-Cl	IIIg	4-Cl
Id	3-Cl	Cl	II d	iBuOC(O)	III d	3,4-Cl	III h	3,4-Cl

## 2.2. Anti-Proliferative Activity Evaluation

We first tested the synthesized compounds for their ability to induce cell death or decrease proliferation in a set of cancer cell lines. We used human cell lines for three major cancer types (glioblastoma U-87 MG, melanoma A-375, metastatic breast cancer MDA-MB-231), and a neuroblastoma SH-SY5Y, which was later intended to be a model in a cytoprotection setting. The cells were incubated with the test compounds overnight, and their proliferation was evaluated using the MTT assay. The compounds were assayed in the concentration range of 1–100  $\mu$ M to account for the lowest potential load for the patient's organism.

All of the compounds from the analogs of EDU series IIIa–h displayed no cytotoxicity for all cell lines tested (Figure 2). On the other hand, all aryl carbamates except IIc were moderately anti-proliferative for all cell lines, decreasing the cell viability by about 40% at 100  $\mu$ M (Figure 3). Pyridyl urea derivatives demonstrated low anti-proliferative activity; the most active of them was Ic (Figure 4).

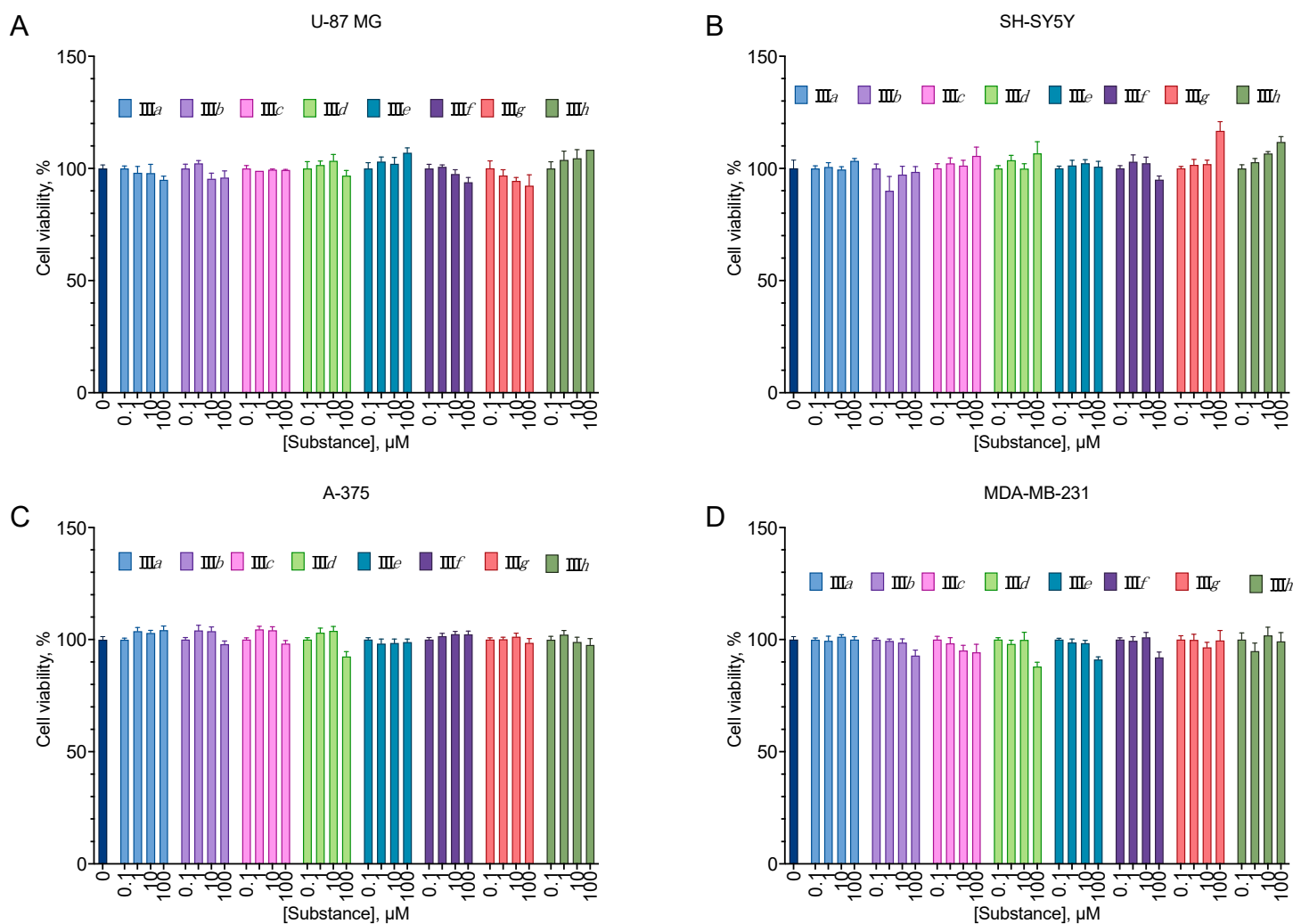


**Figure 2.** Anti-proliferative activity of the compounds **IIIa–h** on the U-87 MG glioblastoma (**A**), SH-SY5Y neuroblastoma (**B**), A-375 melanoma (**C**), and MDA-MB-231 carcinoma (**D**) cell lines. Negative control cells (100% viability) were treated with 0.5% DMSO. Positive control cells (100% cell death) were treated with 3.6  $\mu\text{L}$  of 50% Triton X-100 in ethanol per 200  $\mu\text{L}$  of the cell culture medium. 24 h incubation. MTT test data. Mean  $\pm$  standard error ( $n = 5$  experiments).

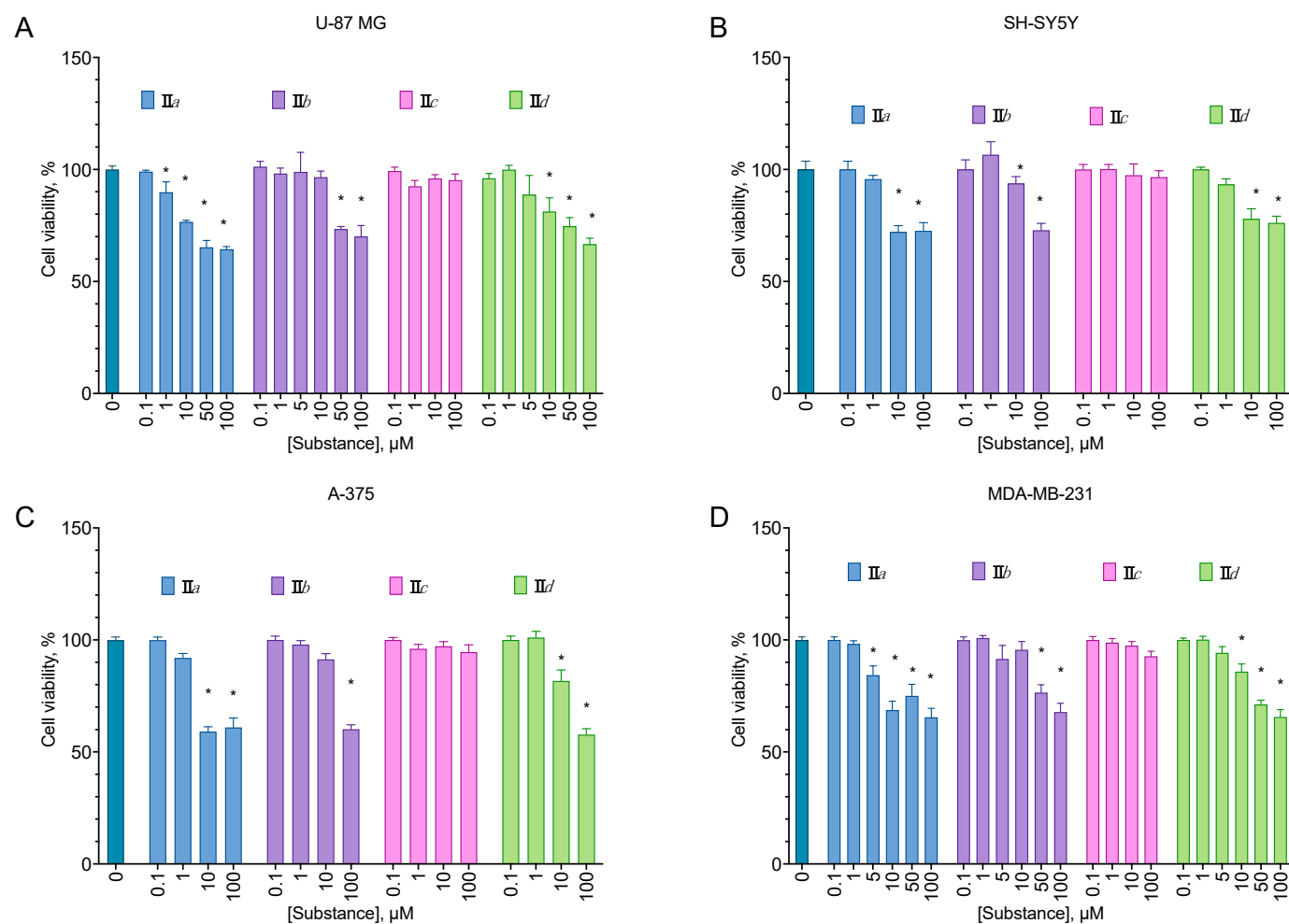


**Figure 3.** Anti-proliferative activity of the aryl carbamates for the U-87 MG glioblastoma (A), SH-SY5Y neuroblastoma (B), A-375 melanoma (C), and MDA-MB-231 carcinoma (D) cell lines. Negative control cells (100% viability) were treated with 0.5% DMSO. Positive control cells (100% cell death) were treated with 3.6  $\mu$ L of 50% Triton X-100 in ethanol per 200  $\mu$ L of the cell culture medium. 24 h incubation. MTT test data. Mean  $\pm$  standard error ( $n = 5$  experiments). \* Statistically significant difference from the control, ANOVA with the Dunnett post-test,  $p \leq 0.05$ .

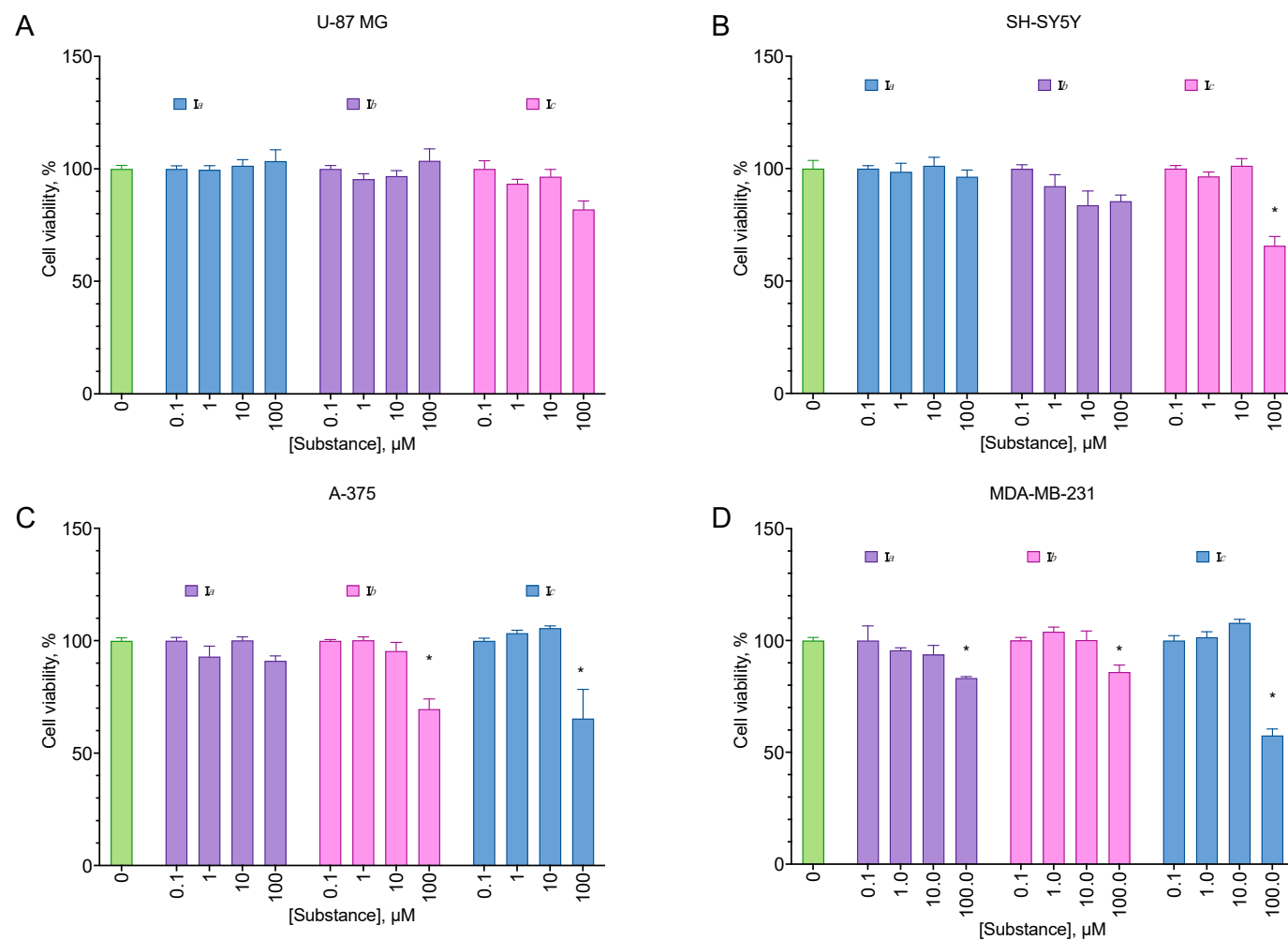


**Figure 4.** Anti-proliferative activity of the pyridyl urea derivatives for the U-87 MG glioblastoma (A), SH-SY5Y neuroblastoma (B), A-375 melanoma (C), and MDA-MB-231 carcinoma (D) cell lines. Negative control cells (100% viability) were treated with 0.5% DMSO. Positive control cells (100% cell death) were treated with 3.6  $\mu\text{L}$  of 50% Triton X-100 in ethanol per 200  $\mu\text{L}$  of the cell culture medium. 24 h incubation. MTT test data. Mean  $\pm$  standard error ( $n = 5$  experiments). \* Statistically significant difference from the control, ANOVA with the Dunnett post-test,  $p \leq 0.05$ .

### 2.3. Selectivity of the Active Arylcarbamates

To investigate substance selectivity, we used normal immortalized human fibroblast cell line Bj-5ta in the same experimental setting as in the cytotoxicity studies. The compounds displayed slight anti-proliferative activity with about 10% cell death at 100  $\mu\text{M}$  of the substance (Figure 5). The selectivity indices were not calculated because of the very low cytotoxicity of the compounds for the Bj-5ta cell line in the designated concentration range. However, at 100  $\mu\text{M}$ , **IIa**, **b** and **d** compounds induced a 32–42% proliferation decrease in the cancer cell lines and only 4–17% in the Bj-5ta cell line. Based on these data, compound selectivity calculated as the anti-proliferative activity ratio at the 100  $\mu\text{M}$  concentration was 2 to 8 (Table 2).

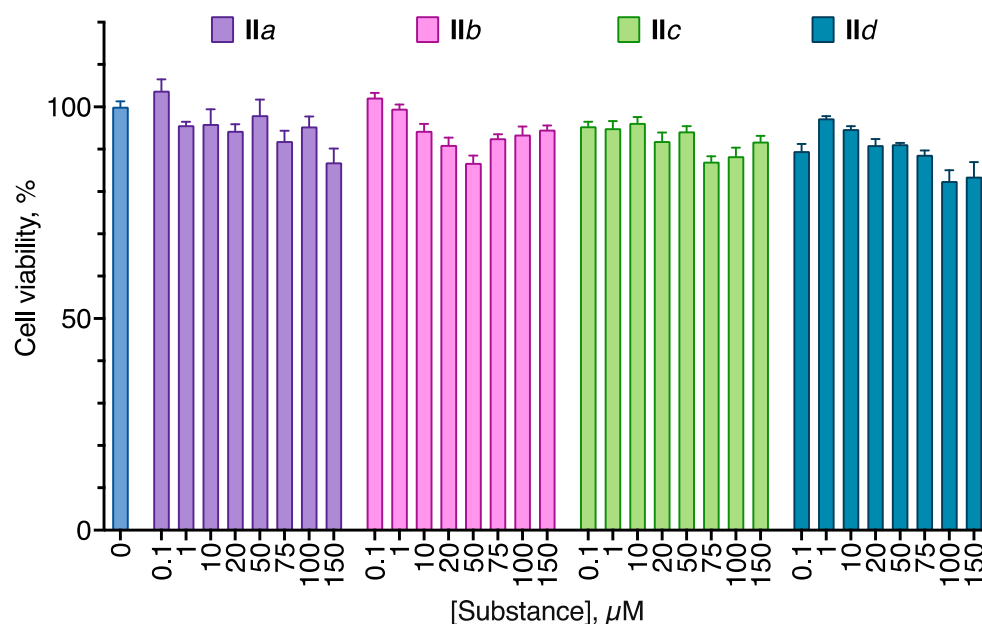


**Figure 5.** Anti-proliferative activity of the aryl carbamates **II** for the human immortalized fibroblast Bj-5ta cell line. Negative control cells (100% viability) were treated with 0.5% DMSO. Positive control cells (100% cell death) were treated with 3.6  $\mu\text{L}$  of 50% Triton X-100 in ethanol per 200  $\mu\text{L}$  of the cell culture medium. 24 h incubation. MTT test data. Mean  $\pm$  standard error ( $n = 3$  experiments).

**Table 2.** Selectivity of the aryl carbamate **II** cytotoxicity for the percent of proliferation decrease at the compound concentration of 100  $\mu\text{M}$ . Incubation time 20 h, MTT assay data, percent of proliferation decrease, mean  $\pm$  standard error ( $n = 5$  experiments). Selectivity was calculated as the anti-proliferative activity ratio for the appropriate cell line to the anti-proliferative activity for the Bj-5ta cell line. ND, not defined.

	A-375		U-87 MG		MDA-MB-231		Bj-5ta
	Proliferation Decrease Mean $\pm$ S.E.	Selectivity	Proliferation Decrease Mean $\pm$ S.E.	Selectivity	Proliferation Decrease Mean $\pm$ S.E.	Selectivity	Proliferation Decrease Mean $\pm$ S.E.
<b>IIa</b>	39 $\pm$ 4.2	8.4	35.6 $\pm$ 1.1	7.7	34.5 $\pm$ 3.9	7.4	4.7 $\pm$ 2.4
<b>IIb</b>	39.8 $\pm$ 1.9	6.1	29.8 $\pm$ 4.8	4.5	32.1 $\pm$ 3.9	4.9	6.6 $\pm$ 1.9
<b>IIc</b>	5.4 $\pm$ 3.2	0.5	4.7 $\pm$ 2.7	0.4	7.3 $\pm$ 2.2	0.6	11.6 $\pm$ 2
<b>IIId</b>	42.3 $\pm$ 2.6	2.4	33.3 $\pm$ 2.6	1.9	34.3 $\pm$ 3.2	2.0	17.5 $\pm$ 2.6

We chose the substance **IIId** as a model to further evaluate the selectivity and cell death type based on the observed anti-proliferative activity.

#### 2.4. Cell Death Type and Mechanism of the Active Arylcarbamates

An investigation of cell death type and mechanism was performed for the **II**d compound on the MDA-MB-231 cell line. Several sets of experiments were performed: (1) cell staining with DNA binding and phosphatidylserine binding dyes with further microscopy to detect necrosis and apoptosis, accordingly; (2) measurement of caspase 3, 8, and 9 activity; (3) measurement of the ability of blockers of necroptosis (necrostatin-1 and necrosulfonate), apoptosis (Z-VAD-FMK), autophagy (hydroxychloroquine), and of a ROS scavenger (N-acetyl cysteine) to prevent **II**d cytotoxicity.

**II**d treatment led to a slight increase in caspase 3 activity and, to some extent, induced phosphatidylserine externalization (Figure 6). Neither of the inhibitors used was able to prevent the cytotoxicity of the compounds, except for the N-acetylcysteine (Figure 7). In accordance with that, the compound induced an increase in the intracellular ROS concentration (Figure 7). However, the inhibition of the ROS-sensitive kinase ASK1 did not reduce the compound's cytotoxicity. These data indicate that the compound induces both apoptosis and necrosis, and possibly slows down cell proliferation.

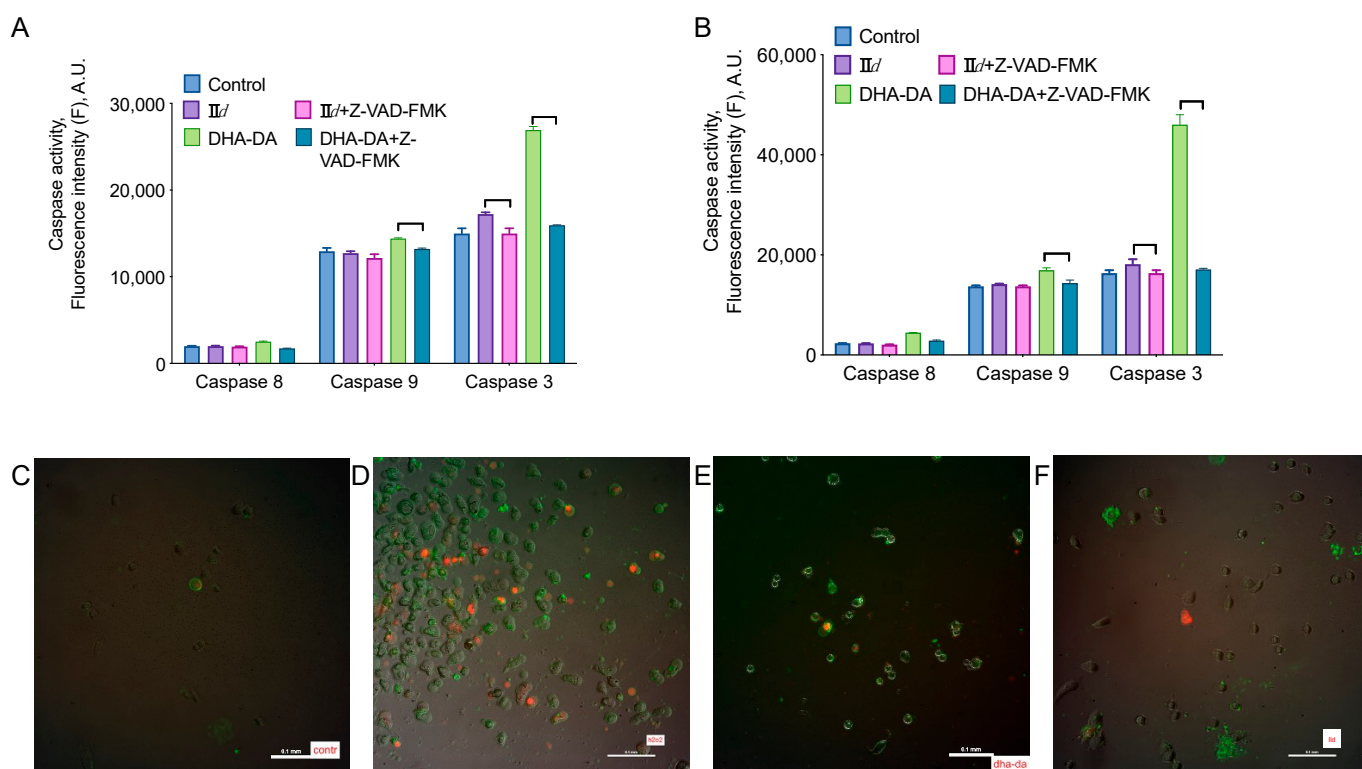


**Figure 6.** Apoptosis induction by the **II**d compound for the MDA-MB-231 cell line. Caspases activity after 5 (A) and 2 (B) h of incubation with 100  $\mu$ M of GT-04 or 90  $\mu$ M of apoptosis inducitor (N-docosahexaenoyl dopamine, DHA-DA) with or without 80  $\mu$ M of Z-VAD-FMK. amalgamated data of  $n = 3$  experiments. Membrane integrity loss (DNA-binding dye propidium iodide, red) and phosphatidylserine externalization (annexin-FITC dye, green) in the control cells (C) and after the treatment with 5 mM of  $H_2O_2$  (D), 80  $\mu$ M of DHA-DA (E) or 100  $\mu$ M of **II**d (F).



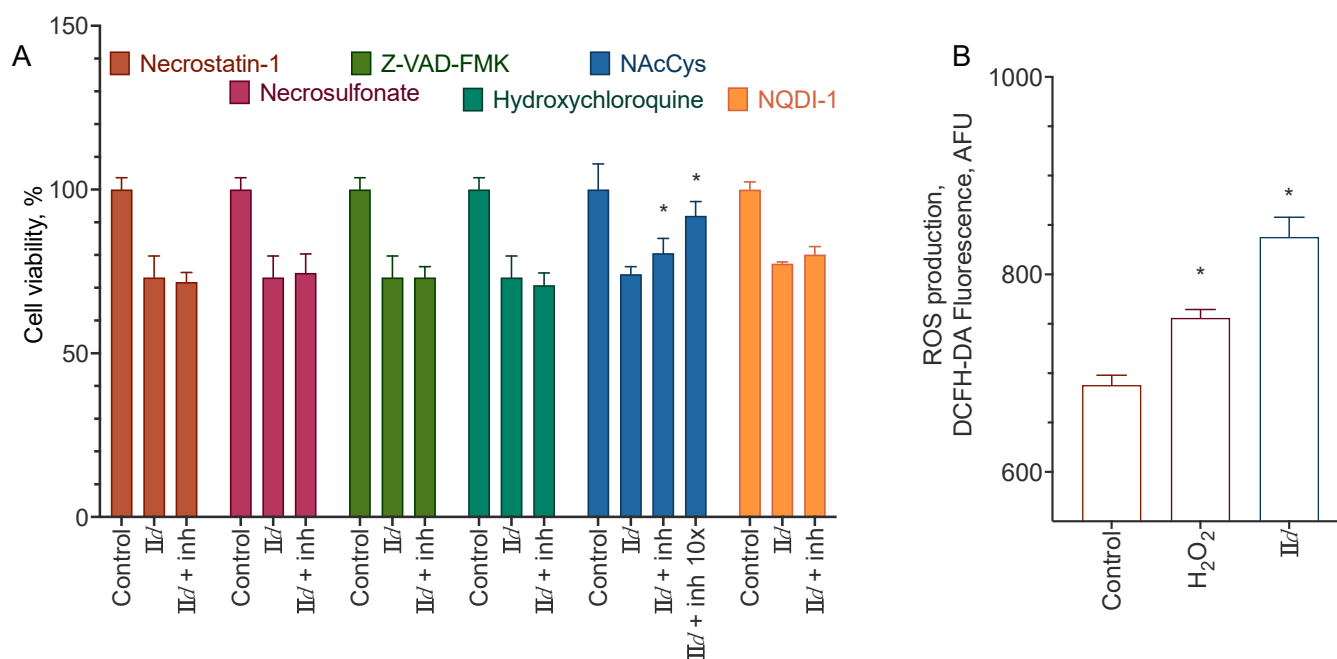


**Figure 7.** Cell death mechanism of the **IIId** compound for the MDA-MB-231 cell line. **(A)** Effect of necroptosis (necrostatin-1, 100  $\mu$ M, and necrosulfonate, 1  $\mu$ M), apoptosis (Z-VAD-FMK, 10  $\mu$ M), autophagy (hydroxychloroquine sulfate, 1  $\mu$ M), and ASK1 (NQDI-1, 10  $\mu$ M) blockers and ROS scavenger (N-Ac-Cys, 0.05 or 0.5 mM + 50 mM HEPES for pH stabilization) on the cytotoxicity of 100  $\mu$ M of **IIId**. 24 h incubation time, MTT assay data, mean  $\pm$  standard error,  $n = 3$  amalgamated experiments. **(B)**, ROS accumulation after the treatment of the cells with 5 mM of H<sub>2</sub>O<sub>2</sub> or 100  $\mu$ M of **IIId**. 24 h incubation time, DCFH-DA fluorescence data,  $n = 3$  amalgamated experiments. \* Statistically significant difference from the control without blocker **(A)** or substance **(B)**, ANOVA with the Tukey post-test,  $p \leq 0.05$ .

### 2.5. Cytoprotection

Based on the data on the cytoprotective activity of the structurally similar compounds [5,19,22,23], we tested the synthesized compounds in two antioxidant models (protection against the H<sub>2</sub>O<sub>2</sub> and CoCl<sub>2</sub> cytotoxicity) in a 24 h incubation. In addition, we evaluated the analogs of EDU **III** for their ability to stimulate cell proliferation after a 72 h treatment. We did not test aryl carbamates **II** and pyridyl ureas **I** for this activity, as these compounds were significantly cytotoxic (Figure 3).

In the cytoprotection experiments, the substances were mainly inactive (Figure 8). However, **IIc** and **IIId** at concentrations from 1 to 10  $\mu$ M were able to increase the cell survival in the CoCl<sub>2</sub> cytotoxicity test by 3 to 8%.

Among the aryl ureas, **III f** exhibited a statistically significant pro-proliferative effect at concentrations of 1–10  $\mu$ M, and **III b**, **c**, and **d** demonstrated anti-proliferative action at the concentration of 100  $\mu$ M (Figure 9).

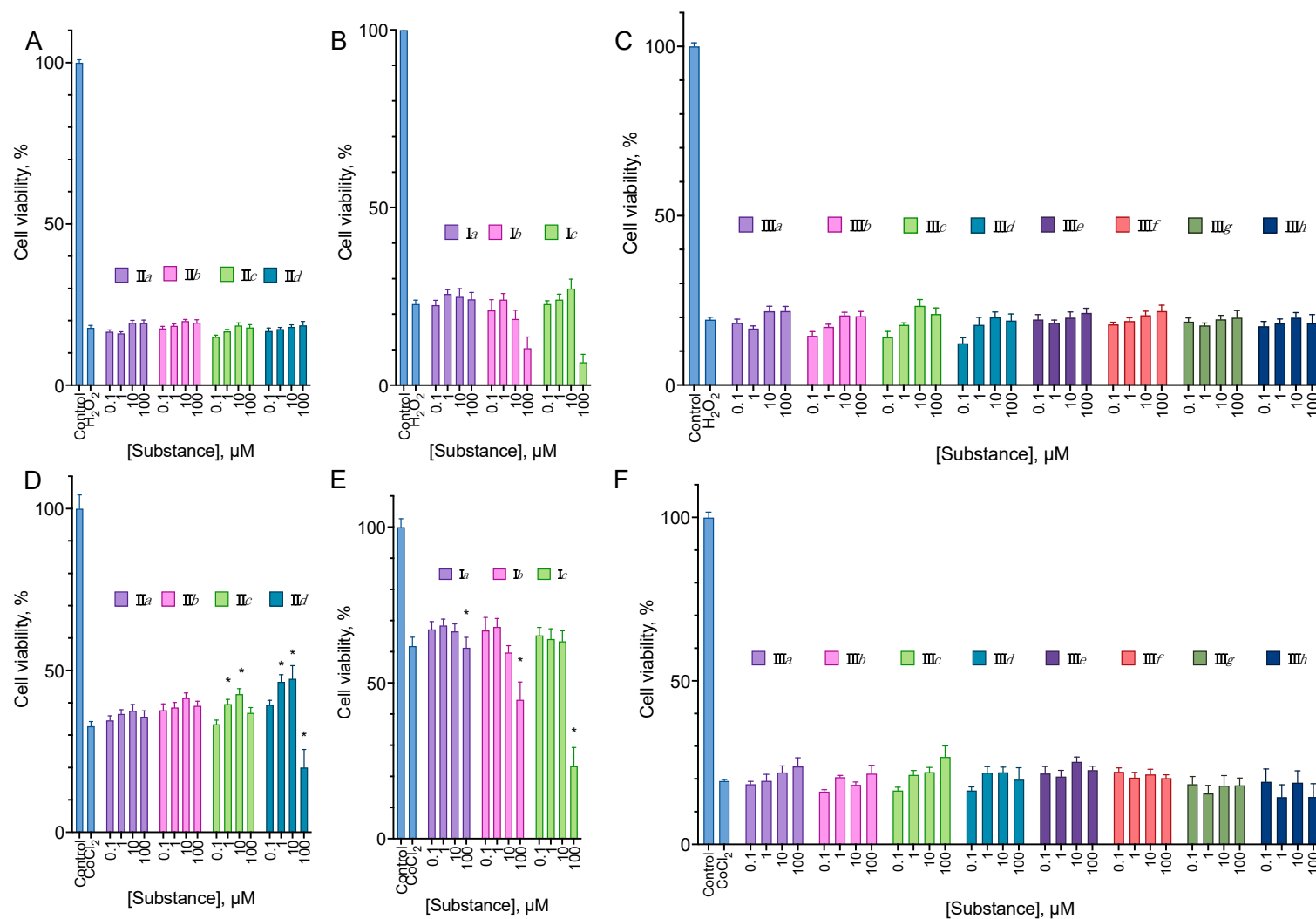


**Figure 8.** The effect of aryl carbamates **II** (A,D) pyridyl ureas **I** (B,E), and EDU analogs **III** (C,F) on the cytotoxicity of H<sub>2</sub>O<sub>2</sub> (A–C) and CoCl<sub>2</sub> (D–F) for the SH-SY5Y cell line. 24 h incubation time. MTT assay data, mean ± standard error,  $n = 3$  amalgamated experiments. \* Statistically significant difference from the control without substance. ANOVA with the Holm-Sidak post-test,  $p \leq 0.05$ .

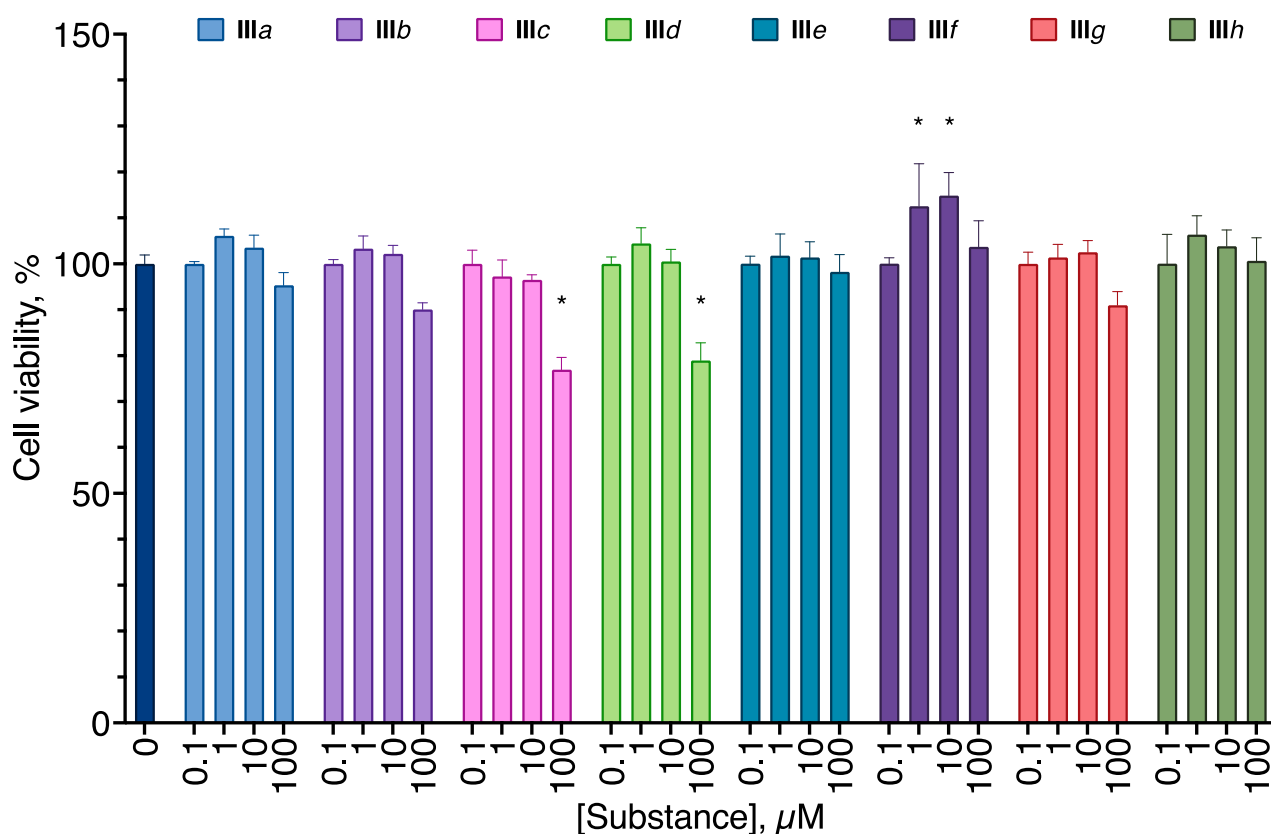


**Figure 9.** EDU analogs **III** effect on the proliferation of SH-SY5Y cell line in a prolonged incubation. Negative control cells (100% viability) were treated with 0.5% DMSO. Positive control cells (100% cell death) were treated with 3.6  $\mu$ L of 50% Triton X-100 in ethanol per 200  $\mu$ L of the cell culture medium. 72 h incubation time. MTT assay data, mean  $\pm$  standard error,  $n = 3$  amalgamated experiments. \* Statistically significant difference from the control without substance. ANOVA with the Dunnett post-test,  $p \leq 0.05$ .

## 2.6. Molecular Docking

Since the compounds demonstrated a substantial anti-proliferative activity with a pro-apoptotic compound, we decided to perform a series of experiments to gain some insights into their molecular targets. We hypothesized that the synthesized compounds and their molecular prototypes cytokinins could share at least some of the receptors.

Cytokinins, the molecular prototypes of the synthesized compounds, have several core molecular targets in mammalian cells: adenosine A2 receptor (A2AR), adenine phosphoribosyltransferase (APRT), and cyclin dependent kinase 2 (CDK2). To probe these proteins as the potential targets for the synthesized compounds, we performed a set of molecular docking experiments using the AutoDock Vina tool. For each protein, several conformation variants were analyzed (A2AR, 5mzj [24], 2ydo [25], and 5mzp [24]; APRT, 6hgs [26], 6hgr [26], and 6hgp [26]; CDK2, 5fp5 [27] and 2jgz [28]).

For A2AR, aryl carbamates **II** typically displayed affinity between the inhibitor caffeine and activator adenosine, while EDU analogs **III** had a lower affinity than both caffeine and adenosine (Figure 10, Tables 3, S2 and S3).

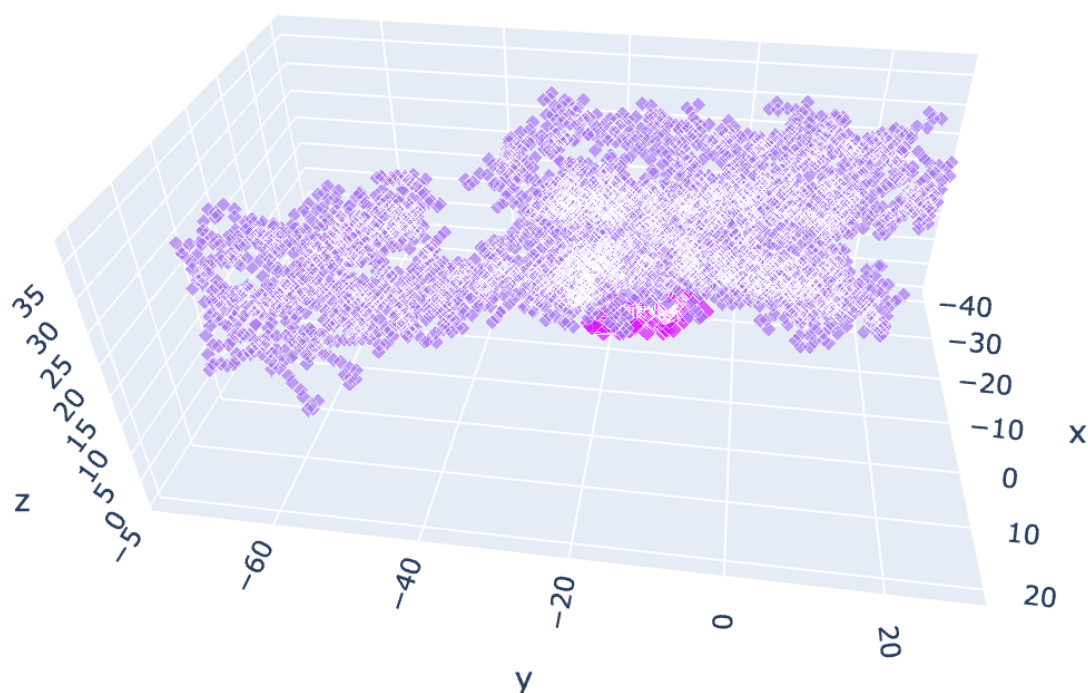


**Figure 10.** Chosen cluster location for the A2AR variant 5mzj. Violet: centroids of the receptor residues. Purple: centroids of the docked molecules.

**Table 3.** Affinity of the synthesized compounds for the adenosine A2 receptor crystal variants. AutoDock Vina data for the most occupied cluster on the protein surface. ND, not present in this cluster. Lower energy means higher affinity.

	A2AR		A2AR + Adenosine		A2AR + Caffeine	
	Energy, Mean $\pm$ S.D.	Occurrence Frequency	Energy, Mean $\pm$ S.D.	Occurrence Frequency	Energy, Mean $\pm$ S.D.	Occurrence Frequency
Adenosine	$-5.37 \pm 0.42$	0.25	$-5.05 \pm 0.47$	0.16	$-5.54 \pm 0.47$	0.1
Caffeine	$-4.53 \pm 0.09$	0.22	ND	ND	$-4.35 \pm 0.10$	0.02
IIa	$-4.87 \pm 0.38$	0.48	$-4.60 \pm 0.48$	0.46	$-4.74 \pm 0.34$	0.32
IIb	$-4.80 \pm 0.38$	0.26	$-4.77 \pm 0.48$	0.31	$-4.61 \pm 0.41$	0.19
IIc	$-4.99 \pm 0.41$	0.3	$-4.81 \pm 0.45$	0.3	$-4.71 \pm 0.30$	0.23
IId	$-4.97 \pm 0.51$	0.45	$-4.79 \pm 0.53$	0.28	$-5.01 \pm 0.34$	0.2
IIIa	$-4.26 \pm 0.46$	0.32	$-3.93 \pm 0.37$	0.33	$-4.38 \pm 0.53$	0.19
IIIb	$-4.26 \pm 0.59$	0.32	$-4.17 \pm 0.51$	0.3	$-4.41 \pm 0.37$	0.27
IIIc	$-4.25 \pm 0.50$	0.25	$-3.91 \pm 0.42$	0.26	$-4.31 \pm 0.38$	0.13
IIId	$-4.28 \pm 0.42$	0.24	$-4.22 \pm 0.40$	0.44	$-4.25 \pm 0.48$	0.23
IIIe	$-4.35 \pm 0.43$	0.23	$-4.33 \pm 0.43$	0.33	$-4.38 \pm 0.40$	0.31
IIIf	$-4.43 \pm 0.48$	0.27	$-4.29 \pm 0.40$	0.33	$-4.47 \pm 0.51$	0.18
IIIg	$-4.58 \pm 0.46$	0.29	$-4.41 \pm 0.40$	0.43	$-4.53 \pm 0.37$	0.21
IIIh	$-4.58 \pm 0.60$	0.26	$-4.46 \pm 0.48$	0.39	$-4.36 \pm 0.31$	0.19

For APRT, the affinity of all compounds was much lower than for the substrate GMP and inhibitor IMP (Figure 11, Tables 4 and S4–S6).

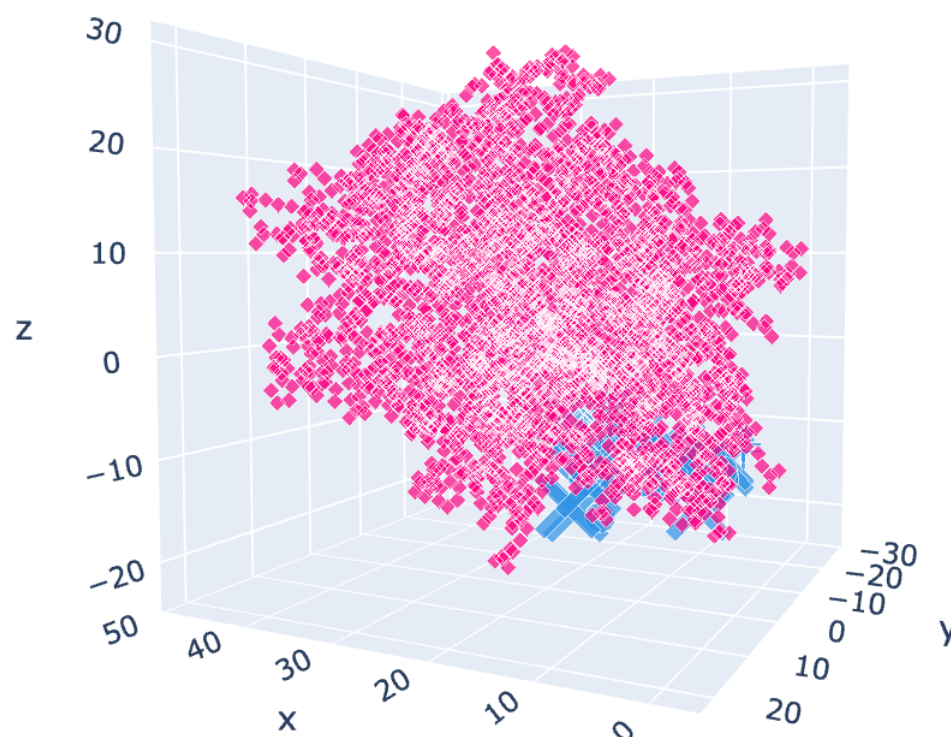


**Figure 11.** Chosen cluster location for the APRT variant 6hgs. Rose: centroids of the receptor residues. Blue: centroids of the docked molecules.

**Table 4.** Affinity of the synthesized compounds for the APRT crystal variants. AutoDock Vina data for the most occupied cluster on the protein surface.

	APRT + GMP		APRT + IMP		APRT + Phosphate	
	Energy, Mean $\pm$ S.D.	Occurrence Frequency	Energy, Mean $\pm$ S.D.	Occurrence Frequency	Energy, Mean $\pm$ S.D.	Occurrence Frequency
GMP	$-6.07 \pm 0.45$	0.18	$-6.16 \pm 0.23$	0.28	$-6.62 \pm 0.42$	0.34
IIa	$-4.57 \pm 0.70$	0.15	$-5.14 \pm 0.55$	0.31	$-4.80 \pm 0.50$	0.14
IIb	$-4.91 \pm 0.81$	0.19	$-4.72 \pm 0.75$	0.19	$-4.90 \pm 0.1$	0.01
IIc	$-4.74 \pm 0.34$	0.12	$-5.07 \pm 0.60$	0.23	$-5.19 \pm 0.58$	0.23
IId	$-4.53 \pm 0.68$	0.1	$-5.41 \pm 0.63$	0.27	$-4.92 \pm 0.36$	0.17
IMP	$-7.43 \pm 0.55$	0.35	$-7.24 \pm 0.49$	0.28	$-7.73 \pm 0.72$	0.13
IIIa	$-4.77 \pm 0.57$	0.23	$-4.33 \pm 0.40$	0.13	$-4.64 \pm 0.79$	0.14
IIIb	$-4.65 \pm 0.55$	0.06	$-4.40 \pm 0.50$	0.32	$-4.25 \pm 0.30$	0.14
IIIc	$-4.60 \pm 0.56$	0.05	$-4.26 \pm 0.40$	0.19	$-4.67 \pm 0.50$	0.14
IIId	$-4.63 \pm 0.51$	0.07	$-4.48 \pm 0.60$	0.22	$-4.64 \pm 0.66$	0.15
IIIe	$-4.41 \pm 0.36$	0.09	$-4.44 \pm 0.53$	0.13	$-4.26 \pm 0.49$	0.07
IIIf	$-4.53 \pm 0.58$	0.12	$-4.35 \pm 0.41$	0.23	$-4.43 \pm 0.32$	0.1
IIIg	$-4.47 \pm 0.33$	0.14	$-4.37 \pm 0.23$	0.09	$-4.39 \pm 0.31$	0.14
IIIh	$-4.50 \pm 0.17$	0.04	$-4.58 \pm 0.62$	0.15	$-4.10 \pm 0.10$	0.05

For CDK2, aryl carbamates **II** displayed affinity close to that of the inhibitor SCP2, and aryl ureas had a much lower affinity (Figure 12, Tables 5, S7 and S8).

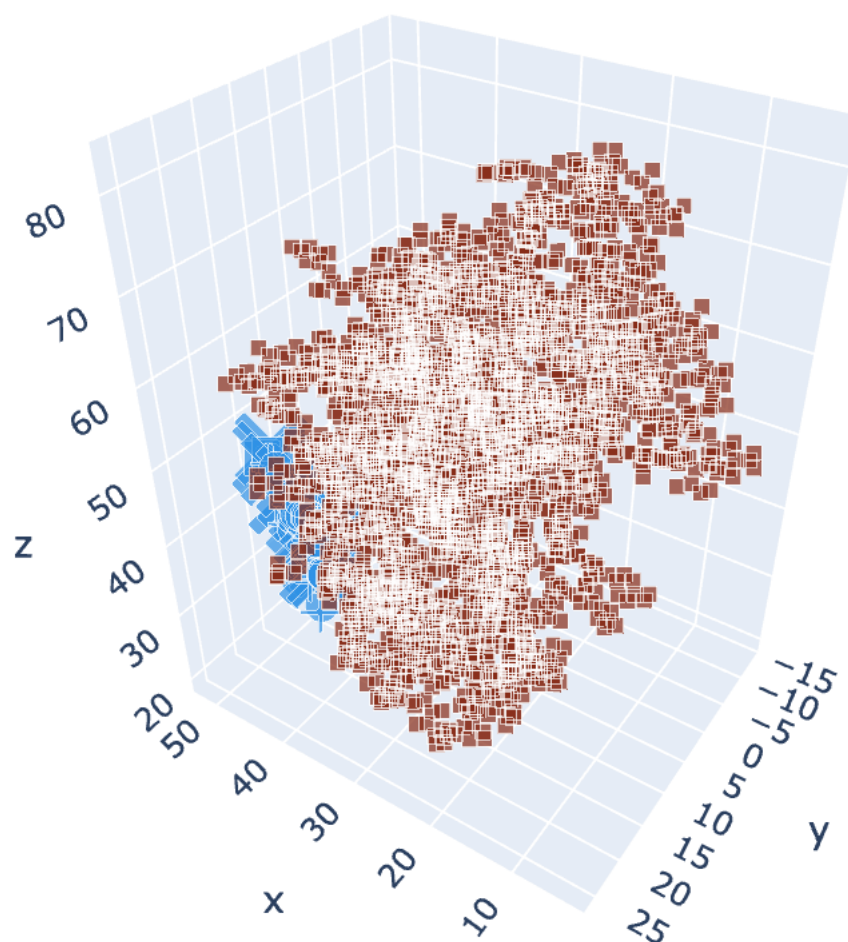


**Figure 12.** Chosen cluster location for the CDK2 variant 5fp5. Brown: centroids of the receptor residues. Blue: centroids of the docked molecules.

**Table 5.** Affinity of the synthesized compounds for the CDK2 crystal variants. AutoDock Vina data for the most occupied cluster on the protein surface.

	CDK2		CDK2 + CyclinB	
	Energy, Mean $\pm$ S.D.	Occurrence Frequency	Energy, Mean $\pm$ S.D.	Occurrence Frequency
<b>IIa</b>	$-4.48 \pm 0.51$	0.18	$-4.87 \pm 0.32$	0.16
<b>IIb</b>	$-4.48 \pm 0.38$	0.14	$-5.09 \pm 0.31$	0.2
<b>IIc</b>	$-4.83 \pm 0.44$	0.19	$-5.21 \pm 0.45$	0.24
<b>IId</b>	$-4.41 \pm 0.38$	0.12	$-5.14 \pm 0.47$	0.2
SCP2	$-4.97 \pm 0.44$	0.18	$-5.68 \pm 0.33$	0.22
<b>IIIa</b>	$-4.13 \pm 0.38$	0.3	$-4.89 \pm 0.66$	0.12
<b>IIIb</b>	$-3.93 \pm 0.35$	0.14	$-4.51 \pm 0.42$	0.1
<b>IIIc</b>	$-3.98 \pm 0.43$	0.14	$-4.27 \pm 0.42$	0.12
<b>IIId</b>	$-4.11 \pm 0.41$	0.18	$-4.59 \pm 0.59$	0.16
<b>IIIe</b>	$-4.39 \pm 0.49$	0.27	$-4.88 \pm 0.44$	0.17
<b>IIIf</b>	$-4.30 \pm 0.61$	0.17	$-4.86 \pm 0.52$	0.22
<b>IIIg</b>	$-4.32 \pm 0.46$	0.19	$-4.68 \pm 0.48$	0.09
<b>IIIh</b>	$-4.54 \pm 0.31$	0.17	$-4.91 \pm 0.54$	0.15

### 3. Discussion

In this paper we report the synthesis and evaluation of some novel pyridyl urea, aryl urea and carbamate derivatives with alkyl and chlorine substitutions for biological activity. The compounds were designed to fill the gap in the known synthetic analogs of the substituted cytokinin-like derivatives. This research continues our earlier study [19], extending it with novel compounds and data on the activity mechanisms. The task looked promising as such compounds are known for exerting cytoprotective and antitumor activity.

To synthesize the designated derivatives, we used known literature methods with the yield in the range of 15 to 55%, which is typical for such compound types.

The synthesized compounds were evaluated for their ability to induce cell death in a set of human cancer cell lines (glioblastoma U-87 MG, melanoma A-375, and metastatic breast cancer MDA-MB-231) chosen based on the clinical significance of the corresponding tumors and on the neuroblastoma SH-SY5Y cell line, which was later intended to be used in the cytoprotection tests. EDU analogs **III** derivatives were not toxic up to the concentration of 100  $\mu\text{M}$  (Figure 2) after 24 h of incubation, but **IIIb**, **c**, **d** and **g** displayed some anti-proliferative activity after 72 h (Figure 9). However, **IIIf** in the latter experiment setting stimulated cell proliferation in SH-SY5Y. Such pro-proliferative activity is quite typical for the cytokinin analogs [5,19,22,23].

Aryl carbamate compounds **II** were anti-proliferative for all cell lines, and three of them demonstrated substantial selectivity compared to the immortalized fibroblast cell line (Table 2). The activity, however, was relatively low for a cytotoxic compound but substantial for an anti-proliferative one, with a 20–40% cell proliferation decrease at a concentration of 100  $\mu\text{M}$ . Pyridyl urea **Ic** was also anti-proliferative, with some preference toward the melanoma and breast cancer cell line (Figure 4). The observed activity was in line with the already described in the literature [29].

Based on the discovered selectivity of the aryl carbamates **II**, we used a set of methods to describe the type of cell death induced by them, with **III d** as the model compound. We used blockers of necroptosis, apoptosis, and autophagy, stained the cells with the apoptosis-sensitive dye, and evaluated the activation of caspases 3, 8, and 9. **III d** induced only a slight increase of caspase 3 activity and apoptotic cell staining, and the only blocker able to decrease its cytotoxicity was the ROS scavenger N-acetyl cysteine. The latter's activity agreed with the **III d** induced accumulation of ROS in the cells (Figure 7). These results point to the primarily anti-proliferative mechanism of the action of the compounds.

To obtain more insights into the molecular mechanism of action of the aryl carbamates **II** and EDU analogs **III**, we performed molecular docking studies with the most known cytokinin analogs targets: adenosine A2 receptor, ARPT, and CDK2 [30,31]. We observed affinities close to those of the known inhibitors toward the A2AR and CDK2 for compounds **II**, and much lower affinities for the compounds **III** (Tables 3 and 5). These results agree with the literature data on the anti-proliferative activity of the inhibitors of these proteins [32,33], but a more detailed study is required to prove this interaction.

Based on the literature data on the ability of the cytokinin derivatives to protect cells against various stress, we tested the synthesized compounds for their ability to protect cells against the cytotoxicity of  $\text{H}_2\text{O}_2$  and  $\text{CoCl}_2$ , and for their ability to stimulate cell proliferation directly. In these experiments, the substances mainly were inactive (Figure 8). However, **IIc** and **d** at concentrations from 1 to 10  $\mu\text{M}$  were able to increase the cell survival in the  $\text{CoCl}_2$  cytotoxicity test by 3 to 8%. Among the aryl ureas, **III f** exhibited a statistically significant pro-proliferative effect at concentrations of 1–10  $\mu\text{M}$ .

The obtained data on the aryl urea, aryl carbamate, and pyridyl urea derivatives demonstrated their ability to inhibit cancer cell proliferation. The probable targets of this activity are adenosine A2 receptor and CDK2, but a more detailed study is required to obtain the molecular details of this interaction.

## 4. Materials and Methods

### 4.1. Materials

L-glutamine, fetal bovine serum, penicillin, streptomycin, amphotericin B, Hanks' salts, Earle's salts, trypsin, DMEM, MEM, and (4,5-dimethylthiazol-2-yl)-2,5-diphenyltetrazolium bromide (MTT) were from PanEco, Moscow, Russia. 2',7'-Dichlorodihydrofluorescein diacetate (DCFH-DA), isopropanol, HCl, CHAPS, protease inhibitor cocktail, EDTA, dithiothreitol, HEPES, DMSO, SCP0139, toluene, acetonitrile, carbon tetrachloride, diethylenetriamine, urea, triethylamine, 4-chlorophenyl isocyanate, 3,4-dichlorophenyl isocyanate, and D-glucose were from Sigma-Aldrich, St. Louis, MO, USA. Hydroxychloroquine, Z-VAD-FMK, necrostatin-1, necrosulfonate, NQDI-1, Ac-DEVD-AFC, and Ac-LEHD-AFC were from Tocris Bioscience, Bristol, UK. The apoptosis assay kit was from Abcam, Cambridge, MA, USA.

Cell lines were purchased from ATCC, Manassas, VA, USA.

### 4.2. Synthesized Compounds' Characterization

Structures of all synthesized compounds were confirmed by  $^1\text{H}$  and  $^{13}\text{C}$  NMR spectroscopy (Figure S1), mass spectrometry and elemental analysis data. The purity of the compounds was confirmed by HPLC-MS and was in the range of 95–99%.  $^1\text{H}$  and  $^{13}\text{C}$  NMR-spectra were recorded with a «Bruker DRX-400» spectrometer operating at 400.13 MHz frequency, using DMSO-*d*<sub>6</sub> as solvent and TMS as an internal standard. Chemical shifts were measured with 0.01 ppm accuracy, coupling constants are reported in Hertz. HPLC-MS was recorded on an inductively coupled plasma mass spectrometer XSeries II ICP-MS (Thermo Scientific Inc., Waltham, MA, USA). Melting point was determined using the melting point (temperature) apparatus Stuart SMP20 (Cole-Palmer, Stone, Staffordshire, UK).

For a qualitative analysis of reaction mixtures compositions, aluminum TLC plates with silica gel (0.015–0.040 mm) with a fluorescent indicator F254 (20 × 20 cm<sup>2</sup>) (Merck Millipore, Darmstadt, Germany) were used. For preparative chromatographic separation of the substances mixtures, «Kieselgel 60» silica gel (0.015–0.040 mm, Merck Millipore, Darmstadt, Germany) was used.

### 4.3. Chemical Synthesis

The preparation of 1-phenyl-3-(4-pyridyl) urea derivatives (**I**) was carried out according to known methods described in the literature [20,21,34]. An amount of 1 eq. of 4-aminopyridine in dry acetone (15 mL per 15 g of substance) was mixed with the solution of relevant phenyl isocyanate in dry acetone (10 mL per 0.5 g of substance). The reaction mixture was held at room temperature for 48 h, then it was concentrated, and the product was purified by column chromatography (silica gel) using Acetone/Chloroform (1:1) followed by crystallization from ethyl acetate.

*N*-(4-pyridyl)-*N'*-phenylurea (**Ia**). 43% yield, mp = 165–167 °C (mp = 162–163 °C [34]).  $^1\text{H}$  NMR (DMSO-*d*<sub>6</sub>,  $\delta$ , ppm, J, Hz): 6.99 (dt, 1H, -C3H-, J = 7.3, 1.0); 7.23–7.31 (m, 2H, -C2H-C3H-C4H-); 7.40 (dd, 2H, -C12H-C-C13H-, J = 4.8, 1.5); 7.44 (dd, 2H, -C1H-C-C5H- J = 8.5, 1.0); 8.33 (d, 2H, -C14H-N-C16H-, J = 6.1); 8.73 (s, 1H, -NH-Ph); 8.97 (s, 1H, -NH-Py). HPLC-MS: [M + 1]<sup>+</sup> found 214.18; calculated value is 214.24.

*N*-(2-chloro-4-pyridyl)-*N'*-2-tolylurea (**Ib**). 54% yield, mp = 189–190 °C (mp = 184–185 °C [34]).  $^1\text{H}$  NMR (DMSO-*d*<sub>6</sub>,  $\delta$ , ppm, J, Hz): 2.23 (s, 3H, CH<sub>3</sub>-); 7.00 (dt, 1H, -C3H-, J = 7.4, 1.0); 7.13–7.19 (m, 2H, -C2H-C3H-C4H-); 7.27 (dd, 1H, -C12H-, J = 5.7, 1.9); 7.64 (d, 1H, -C13H-, J = 1.8); 7.68 (d, 1H, -C5H- J = 7.6); 8.12 (s, 1H, -N7H-); 8.14 (d, 1H, -C16H-, J = 5.6); 9.52 (s, 1H, -N9H-). HPLC-MS: [M + 1]<sup>+</sup> found 262.26; calculated value is 262.07.

*N*-(2-chloro-4-pyridyl)-*N'*-3-tolylurea (**Ic**). 23% yield, mp = 92 °C (mp = 93–95 °C [34]).  $^1\text{H}$  NMR (DMSO-*d*<sub>6</sub>,  $\delta$ , ppm, J, Hz): 2.27 (s, 3H, CH<sub>3</sub>-); 6.82 (d, 1H, -C3H-, J = 7.3); 7.15 (t, 1H, -C4H-, J = 7.7); 7.21 (d, 1H, -C5H-, J = 8.2); 7.28 (m, 1H, -C1H-); 7.29 (dd, 1H, -C12H-, J = 5.7, 1.9); 7.62 (d, 1H, -C13H-, J = 1.8); 8.14 (d, 1H, -C16H-, J = 5.6); 8.77 (s, 1H, -N7H-); 9.22 (s, 1H, -N9H-). HPLC-MS: [M + 1]<sup>+</sup> found 262.26; calculated value is 262.07.



*N*-(2-chloro-4-pyridyl)-*N'*-3-chlorophenylurea (**Id**). 14% yield, mp = 199–200 °C (mp = 198–199 °C [34]). <sup>1</sup>H NMR (DMSO-*d*<sub>6</sub>, δ, ppm, J, Hz): 7.04 (dt, 1H, -C3H-, J = 6.8, 2.1); 7.27–7.33 (m, 3H, -C4H-, -C5H-, -C12H-); 7.60 (d, 1H, -C13H-, J = 1.8); 7.64 (t, 1H, -C1H-, J = 1.8); 8.15 (d, 1H, -C16H-, J = 5.7); 9.04 (s, 1H, -N7H-); 9.31 (s, 1H, -N9H-). HPLC-MS: [M + 1]<sup>+</sup> found 282.25; calculated value is 282.12.

Compounds from the **II**-series were synthesized according to refs. [9,10].

*O*-*i*-Propyl-*N*-(2-hydroxyethylamino)carbamate (**IIa**) was synthesized according to known procedures [35].

Briefly, for the oxamate derivatives, a solution of 1 eq. of *O*-alkyl-*N*-(2-hydroxyethyl)oxamate in dry toluene (15 mL per 2 g of substance) was placed in a round bottom flask equipped with a calcium chloride tube and magnetic stirrer. Then, the solution of 1 eq. 4-methyl phenyl isocyanate in dry toluene (30 mL per 1.5 g of isocyanate) and 2–3 drops of triethylamine were added. The reaction mixture was stirred at room temperature for 15 min, wherein precipitation was formed. The resulting precipitate was filtered off. The product was purified by recrystallization from isopropanol.

*O*-Propyl-*N*-[2-(4-methylphenylaminocarbonyloxy)ethyl]oxamate (**IIb**). 35% yield, mp = 123–125 °C. <sup>1</sup>H NMR (DMSO-*d*<sub>6</sub>, δ, ppm, J, Hz): 0.92 (t, 3 H, CH<sub>3</sub>, J<sub>3</sub> = 8.0); 1.63 (sextet, 2 H, CH<sub>2</sub>CH<sub>3</sub>, J<sub>3</sub> = 8); 2.28 (s, 3 H, CH<sub>3</sub>CH<sub>arom</sub>); 3.85–4.13 (m, 6 H, CH<sub>2</sub>O, CH<sub>2</sub>NH, CH<sub>2</sub>OCO); 7.01 (d, 2 H, m-CH<sub>arom</sub>, J<sub>3</sub> = 8.0); 7.14 (d, 2 H, o-CH<sub>arom</sub>, J<sub>3</sub> = 8.0); 9.08 (bs, 1 H, NHCOO); 9.47 (bs, 1 H, NHCOO). <sup>13</sup>C NMR (DMSO-*d*<sub>6</sub>, δ, ppm): 10.60 (CH<sub>3</sub>CH<sub>2</sub>); 20.78 (CH<sub>3</sub>CH<sub>2</sub>); 21.73 (CH<sub>3</sub>Carom); 62.36 (CH<sub>2</sub>NH); 67.85 (CH<sub>2</sub>OCONH); 68.36 (CH<sub>2</sub>OCO); 118.66 (CH<sub>3</sub>Carom); 131.69 (m-CH<sub>arom</sub>); 136.85 (o-CH<sub>arom</sub>); 137.64 (ipso-Carom); 153.74 (CONH); 157.63 (OCNH); 161.03 (OCO). HPLC-MS: [M + 1]<sup>+</sup> found 309.30.; calculated value is 309.14.

*O*-Isobutyl-*N*-[2-(4-methylphenylaminocarbonyloxy)ethyl]oxamate (**IIc**). 55% yield, mp = 205–210 °C. <sup>1</sup>H NMR (DMSO-*d*<sub>6</sub>, δ, ppm, J, Hz): 0.91 (d, 6 H, CH<sub>3</sub>, J<sub>3</sub> = 6.2); 1.96 (septet, 1 H, CHCH<sub>3</sub>, J<sub>3</sub> = 6.4); 2.24 (s, 3 H, CH<sub>3</sub>CH<sub>arom</sub>); 3.45 (bs, 2 H, CH<sub>2</sub>O); 3.99 (d, 2 H, CHCH<sub>2</sub>O, J<sub>3</sub> = 6.2); 4.18 (t, 2 H, CH<sub>2</sub>NH, J<sub>3</sub> = 5.0); 7.08 (d, 2 H, m-CH<sub>arom</sub>, J<sub>3</sub> = 7.7); 7.33 (d, 2 H, o-CH<sub>arom</sub>, J<sub>3</sub> = 7.5); 9.04 (bs, 1 H, NHCOO); 9.57 (bs, 1 H, NHCOO). <sup>13</sup>C NMR (DMSO-*d*<sub>6</sub>, δ, ppm): 19.18 (CH<sub>3</sub>); 20.78 (CH<sub>3</sub>Carom); 27.58 (CHCH<sub>3</sub>); 54.67 (CHCH<sub>2</sub>O); 62.37 (CH<sub>2</sub>NH); 72.06 (CH<sub>2</sub>O); 118.69 (CH<sub>3</sub>Carom); 129.63 (m-CH<sub>arom</sub>); 131.00 (o-CH<sub>arom</sub>); 136.94 (ipso-Carom); 153.84 (CONH); 157.69 (OCNH); 161.04 (OCO). HPLC-MS: [M + 1]<sup>+</sup> found 323.10; calculated value is 323.15.

The synthesis of the compound **IIc** is described in the literature [9,10].

Compounds from the **III**-series were synthesized according to ref. [19].

Briefly, for the aryl carbamates (**IIIa, b, c, d**) synthesis, 1 eq. of 2-hydroxyethyl derivative in a small volume of dry acetonitrile (20 mL per 1 g of substance) was placed in a round bottom flask equipped with a calcium chloride tube and magnetic stirrer. Then, a solution with 1 eq. of the relevant phenyl isocyanate in dry acetonitrile (30 mL per 1 g of substance) and 2–3 drops of triethylamine were added. The reaction mixture was stirred at room temperature for 24 h. The solution was evaporated to dryness, and the residue was recrystallized from methanol and from isopropanol. The precipitate was filtered off and washed with a small amount of cold isopropanol.

2-(2-oxoimidazolidin-1-yl) ethyl-*N*-phenyl carbamate (**IIIa**). 15% yield, mp = 115–117 °C. <sup>1</sup>H NMR (DMSO-*d*<sub>6</sub>, δ, ppm, J, Hz): 3.17–3.26 (m, 2H, -N-CH<sub>2</sub>-CH<sub>2</sub>-cycle); 3.29–3.34 (m, 2H, -N-CH<sub>2</sub>-CH<sub>2</sub>-cycle); 3.38–3.45 (m, 2H, -N-CH<sub>2</sub>-CH<sub>2</sub>-O-); 4.13–4.18 (m, 2H, -N-CH<sub>2</sub>-CH<sub>2</sub>-O-); 6.21 (s, 1H, -NH-C(O)-N-); 6.97 (tt, 1H, CH<sub>aryl</sub>, J = 7.4, 0.9); 7.18–7.32 (m, 2H, CH<sub>aryl</sub>); 7.39–7.47 (m, 2H, CH<sub>aryl</sub>); 9.50 (s, 1H, -NH-C(O)-O-). HPLC-MS: [M + 1]<sup>+</sup> 250.24; calculated value is 250.27.

2-(2-oxoimidazolidin-1-yl)ethyl-*N*-(3-chlorophenyl) carbamate (**IIIb**). 35% yield, mp = 112–114 °C. <sup>1</sup>H NMR (DMSO-*d*<sub>6</sub>, δ, ppm, J, Hz): 3.19–3.22 (m, 2H, -N-CH<sub>2</sub>-CH<sub>2</sub>-cycle); 3.28–3.33 (m, 2H, -N-CH<sub>2</sub>-CH<sub>2</sub>-cycle); 3.37–3.43 (m, 2H, -N-CH<sub>2</sub>-CH<sub>2</sub>-O-); 4.16 (t, 2H, -N-CH<sub>2</sub>-CH<sub>2</sub>-O-, J = 5.1); 6.36 (s, 1H, -NH-C(O)-N-); 7.02 (m, 1H, CH<sub>aryl</sub>); 7.28

(m, 1H, CHaryl); 7.36 (m, 1H, CHaryl); 7.59 (m, 1H, CHaryl); 9.89 (s, 1H, -NH-C(O)-O-). HPLC-MS: [M + 1]<sup>+</sup> 284.20; calculated value 284.07

For the compounds **IIIc** and **III d** see ref. [19].

Briefly, for the aryl ureas (**IIIe, f, g, h**) synthesis 1 eq. of amine in dry toluene (50 mL per 4 g of substance) was placed in a three-necked flask with a thermometer, a dropping funnel, and a magnetic stirrer. The mixture was cooled in an ice bath to a temperature no higher than 5 °C. Then, a solution with 1 eq. of the relevant phenyl isocyanate in dry toluene (50 mL per 3.5–4 g of substance) was added dropwise with stirring, keeping a temperature no higher than 5 °C. The reaction mixture was stirred at room temperature for 24 h. The precipitate was filtered off and recrystallized from acetone.

*N*-[2-(2-oxoimidazolidin-1-yl)ethyl]-*N'*-(3-chlorophenyl) urea (**III f**). 16% yield, mp = 137–138 °C. <sup>1</sup>H NMR (DMSO-*d*<sub>6</sub>, δ, ppm, J, Hz): 3.12 (t, 2H, -N-CH<sub>2</sub>-CH<sub>2</sub>-cycle, J = 5.8); 3.17–3.25 (m, 2H, -N-CH<sub>2</sub>-CH<sub>2</sub>-NH); 3.33–3.39 (m, 2H, -N-CH<sub>2</sub>-CH<sub>2</sub>-NH); 6.134 (t, 1H, -NH-C(O)-NH); 6.17 (s, 1H, -NH-C(O)-N); 6.87–6.92 (m, 1H, CHaryl); 7.13–7.24 (m, 2H); 7.63 (t, 1H, CHaryl, J = 1.8); 8.66 (s, 1H, -NH-C(O)-NH). HPLC-MS: [M + 1]<sup>+</sup> found 283.29; calculated value is 283.09.

The compounds **IIIe, g, h** are described in the literature [19].

#### 4.4. Cell Culture

All cell lines were maintained in a CO<sub>2</sub> incubator at 37 °C, 95% humidity and 5% CO<sub>2</sub>. The composition of the culture medium for the cells was as follows: MDA-MB-231 (ATCC HTB-26), Bj-5ta (ATCC CRL-4001), and A-375 (ATCC CRL-1619): DMEM, 4 mM L-Gln, 10% fetal bovine serum (FBS), U-87 MG (ATCC HTB-14): MEM, 2 mM L-Gln, 1% non-essential amino acids, 1 mM pyruvate, and 10% FBS; SH-SY5Y (ATCC CRL-2266): 1:1 MEM: F12, 10% FBS, 2 mM L-Gln, 0.5 mM sodium pyruvate, 0.5% non-essential amino acids. The cells were routinely checked for mycoplasma contamination using RT-PCR. All cell media contained 100 U/mL penicillin, 100 µg/mL streptomycin, and 2.5 µg/mL amphotericin B. The cells were passaged using Trypsin-EDTA solution (PanEco, Moscow, Russia), the continuous passaging time did not exceed 40 passages.

Mycoplasma contamination was controlled using the Mycoplasma Detection Kit (Jena Bioscience, Jena, Germany).

#### 4.5. Oxidative Stress Induction

For cell viability experiments, the cells were seeded at a density of 30,000 per well of a 96-well plate in 100 µL of the test medium (culture medium with 50 mM HEPES, pH 7.4, and without serum and pyruvate) and incubated for 12 h. After that, a substance solution with or without the toxic agent in 100 µL fresh test medium was added to the medium present in the wells and incubated for 24 h, after which cell viability was measured using the MTT assay. Cytotoxicity was induced by either 100 µM of H<sub>2</sub>O<sub>2</sub> or 700 µM of CoCl<sub>2</sub> (from the freshly prepared stock in EtOH).

#### 4.6. Cytotoxicity and Proliferation Stimulation

For analysis of cell death induction and ROS generation, the cells were plated in 96-well plates at a density of  $1.5 \times 10^4$  cells for the cytotoxicity assay and 8000 for the proliferation study per well and grown overnight. The dilutions of the test compounds prepared in DMSO and dissolved in the culture medium (without serum starvation) were added to the cells in triplicate for each concentration (100 µL of the fresh medium with the substance to 100 µL of the old medium in the well) and incubated for 18 h in the case of cytotoxicity and 72 h in the case of the proliferation stimulation. The incubation time was chosen based on the most pronounced differences between the compounds tested. The final DMSO concentration was 0.5%. Negative control cells (100% viability) were treated with 0.5% DMSO. Positive control cells (100% cell death) were treated with 3.6 µL of 50% Triton X-100 in ethanol per 200 µL of the cell culture medium. Separate controls were without DMSO (no difference with the control 0.5% DMSO was found). Depending

on the experiment series, the effects of the test substances on the cell viability and ROS production were evaluated using the MTT assay and DCFH-DA, accordingly.

#### 4.7. Cell Viability Assay

Cell viability was analyzed using the MTT test [36]. In short, the culture medium was removed from the wells and 75  $\mu$ L of the 0.5 mg/mL solution of MTT with 1 g/L D-glucose in Earle's salts was added to each well and incubated for 90 min in the CO<sub>2</sub> incubator at 37 °C. After that, 75  $\mu$ L of 0.04 M HCl in isopropanol was added to the MTT solution in each well and incubated on a plate shaker at 37 °C for 30 min. The optical density of the solution was determined using a Hidex Sense Beta Plus microplate reader (Hidex, Turku, Finland) at the wavelength of 570 nm with a reference wavelength of 620 nm.

#### 4.8. Apoptosis Assay

Apoptosis level was analyzed using an Apoptosis/Necrosis detection kit (ab176749, Abcam, Cambridge, UK). The cells were seeded at a density of 15,000 per well of a 96-well plate and grown for 12 h. After that, 475  $\mu$ M of H<sub>2</sub>O<sub>2</sub> alone or with the peptide was added in 100  $\mu$ L of the fresh medium to 100  $\mu$ L of the old medium in the wells and incubated for 1 h at 37 °C in a CO<sub>2</sub> incubator. After that, the medium was removed, and the cells were stained according to the manufacturer's instructions using the phosphatidylserine sensor (apoptotic cells, green fluorescence) and membrane-impermeable dye 7-AAD (necrotic cells, red fluorescence). The stained cells were photographed using an inverted fluorescent microscope Nikon Ti-S using a Semrock GFP-3035D filter cube with magnification 100 $\times$ . For each well, five non-intersecting view fields were captured, and apoptotic cells were counted.

#### 4.9. Caspase Activity Assay

The determination of caspase activity was performed using the specific substrates with a fluorescent 7-amido-4-trifluoromethylcoumarin (AFC) label. Cells were seeded into a 96-well plate ( $7 \times 10^4$  cells/well) and incubated overnight. Test compound solutions in the full culture medium were added to the cells without medium change and incubated in a CO<sub>2</sub> incubator for 4 h at 37 °C. A pan-caspase inhibitor Z-VAD-FMK (80  $\mu$ M) was used as a negative control. Then, the medium was discarded and 120  $\mu$ L of the caspase assay buffer (20 mM HEPES, 2 mM EDTA, 0.1% CHAPS, 5 mM dithiothreitol, protease inhibitor cocktail, pH 7.4) was added to the cells. Then, the cells were frozen at  $-50$  °C. After thawing, 120  $\mu$ L of the caspase substrates Ac-DEVD-AFC (32  $\mu$ M), Ac-LEHD-AFC (32  $\mu$ M), and SCP0139 (32  $\mu$ M) were added to the cell lysates and incubated for 90 min at 37 °C. The released AFC determination was performed using the Hidex Sense Beta Plus microplate reader (Hidex, Turku, Finland) at  $\lambda_{\text{ex}} = 505$  nm,  $\lambda_{\text{em}} = 400$  nm.

#### 4.10. ROS Assay

ROS generation was measured using the DCFH-DA dye. The cells were seeded at a density of 60,000 per well of a 96-well plate and grown for 12 h. After that, the cells were treated with the substances in the culture medium for 24 h. Cells treated with a medium without H<sub>2</sub>O<sub>2</sub> and substances were used as a control. After that, the medium was replaced with a fresh one with 25  $\mu$ M of the dye, and the cells were incubated in the CO<sub>2</sub> incubator at 37 °C for 1 h. After the incubation, the cells were washed twice with Earle's balanced salt solution, and the fluorescence was measured using the plate reader Hidex Sense Beta Plus (Hidex, Turku, Finland),  $\lambda_{\text{ex}} = 490$  nm,  $\lambda_{\text{em}} = 535$  nm.

#### 4.11. Molecular Docking

Ligand structures were obtained from the PubChem database (<https://pubchem.ncbi.nlm.nih.gov/>, access date 1 May 2022) or prepared manually using Avogadro 1.93.0 software and optimized using the OpenBabel 3.0.0 software (<http://openbabel.org/>, access date 1 May 2022) [37] using the FFE force field with Fastest descent and  $dE \leq 5 \times 10^{-6}$  threshold.

Protein structures were obtained from the PDB database (<https://www.rcsb.org/>, access date 1 May 2022) and optimized using the Chiron service (<https://dokhlab.med.psu.edu/chiron/processManager.php>, access date 01.05.2022) [38]. Molecular docking was performed using the AutoDock Vina 1.1.2 (<http://vina.scripps.edu/>, access date 1 May 2022) [39]. To detect possible alternative binding sites and compare the affinities of the ligands for them, the procedure described in the literature [40] was used. As such, molecular docking was performed in two steps: first, we docked each molecule to the whole receptor as one large binding area to locate potential alternative binding sites, then the coordinates of the docking results were clustered and averaged to give the centers of the binding sites. The grid center coordinates are represented in the Table 6. For large proteins, several grid centers were used to cover the whole protein. In all cases, the grid size was  $126 \times 126 \times 126 \text{ \AA}$ , chosen to cover the whole protein, and exhaustiveness was set to 16. For each ligand, the docking was performed 10 times with different random seeds generating 10 conformations each time. The resulting coordinates were clustered using the OPTICS algorithm [41] from the package scikit-learn [42].

**Table 6.** Grid centers of the docking experiments.

Protein	Configuration Variant	x	y	z
A2AR 5mzj	1	−17.629	−30.760	18.168
	2	−4.629	−50.760	18.168
	3	−17.629	6.760	18.168
A2AR 2ydo	1	−23.602	10.545	−25.256
	2	−23.602	20.545	−25.256
	3	−4.629	−50.760	18.168
A2AR 5mzp	1	−16.417	−40.474	18.316
	2	−16.417	5.474	18.316
	3	−1.417	−50.474	18.316
APRT 6hgs	1	22.572	−3.082	4.313
APRT 6hgr	1	23.667	−7.067	5.057
APRT 6hgp	1	−24.642	0.247	1.919
CDK2 5fp5	1	29.547	4.964	49.678
CDK2 2jgz	1	55.623	20.504	−10.503
	2	38.623	20.504	5.503
	3	38.623	20.504	−30.503

#### 4.12. Statistics

All experiments were performed at least in triplicate. Statistical analysis was performed with the GraphPad Prism 9.0 software using ANOVA with the Holm-Sidak or Tukey post-tests;  $p \leq 0.05$  was considered a statistically significant difference.

## 5. Conclusions

In this paper we report the synthesis of some aryl carbamate, pyridyl urea, and aryl urea derivatives with alkyl and chlorine substitutions and tests of their cytotoxic and cytoprotective activity. Aryl carbamates with an oxamate moiety were anti-proliferative for the cancer cell lines tested, while the aryl ureas were inactive. In the cytoprotection studies, aryl carbamates were able to counteract the  $\text{CoCl}_2$  cytotoxicity by 3–8%. The possible molecular targets of the aryl carbamates with oxamate moiety during the anti-proliferative action were the adenosine A2 receptor and CDK2.

The novelty of the research was the screening of the chemically synthesized cytokinin analogs, which have never been characterized for such biological activity before. Although most of the compounds displayed little activity in the most tests, compounds of the series **II** displayed an interesting highly selective antiproliferative capacity. This activity was observed, among others, for the glioblastoma cell line. Given the lack of efficient treatments for this cancer type, such activity could be used in the combined or supporting therapy after additional research.

**Supplementary Materials:** The following supporting information can be downloaded at: <https://www.mdpi.com/article/10.3390/molecules27113616/s1>. Figure S1: NMR spectroscopy data for the synthesized compounds. Table S1: Affinities of the clusters for the A2AR receptor variant 5mzj. Table S2: Affinities of the clusters for the A2AR receptor variant 2ydo. Table S3: Affinities of the clusters for the A2AR receptor variant 5mzp. Table S4: Affinities of the clusters for the APRT variant 6hgs. Table S5: Affinities of the clusters for the APRT variant 6hgr. Table S6: Affinities of the clusters for the APRT variant 6hgp. Table S7: Affinities of the clusters for the CDK2 variant 5fp5. Table S8: Affinities of the clusters for the CDK2 variant 2jgz.

**Author Contributions:** Conceptualization, M.A. and M.O.; methodology, M.O. and M.A.; software, M.A. and A.A.; validation, M.O., L.K., A.K. and M.A.; formal analysis, M.A.; investigation, M.I., G.S., P.D., A.C. and A.A.; resources, L.K.; data curation, M.A.; writing—original draft preparation, M.O. and M.A.; writing—review and editing, M.O. and L.K.; visualization, M.A.; supervision, L.K.; project administration, M.O. and A.K.; funding acquisition, M.O. All authors have read and agreed to the published version of the manuscript.

**Funding:** The study was supported by a grant of Ministry of Science and Higher Education of Russian Federation No. 075-15-2020-792 (Unique identifier RF 190220 × 0031).

**Institutional Review Board Statement:** Not applicable.

**Informed Consent Statement:** Not applicable.

**Data Availability Statement:** The data presented in this study are available on request from the corresponding author. The data are not publicly available due to legal issues.

**Conflicts of Interest:** The authors declare no conflict of interest. The funders had no role in the design of the study; in the collection, analyses, or interpretation of data; in the writing of the manuscript, or in the decision to publish the results.

**Sample Availability:** Samples of all the synthesized compounds are available from the authors.

## References

1. Duszka, K.; Clark, B.; Massino, F.; Barciszewski, J. Biological Activities of Kinetin. In *Herbal Drugs: Ethnomedicine to Modern Medicine*; Springer: Berlin/Heidelberg, Germany, 2009. [CrossRef]
2. Sun, J.-H.; Liu, Y.-M.; Cao, T.; Ouyang, W.-Q. Effect of kinetin on ovary and uterus in D-galactose-induced female mouse model of aging. *Sheng Li Xue Bao* **2013**, *65*, 389–394. [PubMed]
3. Kim, S.W.; Goossens, A.; Libert, C.; Van Immerseel, F.; Staal, J.; Beyaert, R. Phytohormones: Multifunctional Nutraceuticals against Metabolic Syndrome and Comorbid Diseases. *Biochem. Pharmacol.* **2020**, *175*, 113866. [CrossRef] [PubMed]
4. Voller, J.; Maková, B.; Kadlecová, A.; Gonzalez, G.; Strnad, M. Plant Hormone Cytokinins for Modulating Human Aging and Age-Related Diseases. In *Hormones in Ageing and Longevity*; Springer: Cham, Switzerland, 2017; pp. 311–335; ISBN 978-3-319-63001-4.
5. Oshchepkov, M.S.; Kalistratova, A.V.; Savelieva, E.M.; Romanov, G.A.; Bystrova, N.A.; Kochetkov, K.A. Natural and Synthetic Cytokinins and Their Applications in Biotechnology, Agrochemistry and Medicine. *Russ. Chem. Rev.* **2020**, *89*, 787–810. [CrossRef]
6. Kalistratova, A.V.; Kovalenko, L.V.; Oshchepkov, M.S.; Solovieva, I.N.; Polivanova, A.G.; Bystrova, N.A.; Kochetkov, K.A. Biological Activity of the Novel Plant Growth Regulators: N-Alkoxy-carbonylaminoethyl-N'-Arylureas. *Bulg. J. Agric. Sci.* **2020**, *26*, 772–776.
7. Okamoto, T.; Shudo, K.; Isogai, Y. Structural and biological links between urea and purine cytokinins. In *Pesticide Chemistry: Human Welfare and Environment*; Doyle, P., Fujita, T., Eds.; Elsevier Ltd.: Pergamon, Turkey, 1983; pp. 333–338. ISBN 978-0-08-029222-9.
8. Okamoto, T.; Shudo, K.; Takahashi, S.; Kawachi, E.; Isogai, Y. 4-Pyridylureas Are Surprisingly Potent Cytokinins. The Structure-Activity Relationship. *Chem. Pharm. Bull.* **1981**, *29*, 3748–3750. [CrossRef]
9. Kalistratova, A.V.; Oshchepkov, M.S.; Ivanova, M.S.; Kovalenko, L.V.; Tsvetkova, M.A.; Bystrova, N.A.; Kochetkov, K.A. Wheat (*Triticum aestivum* L.) Reaction to New Bifunctional Carbamate Compounds. *J. Agric. Sci.* **2021**, *13*, 36. [CrossRef]

10. Vorob'ev, M.M.; Khomenkov, V.S.; Sinitsyna, O.V.; Levinskaya, O.A.; Kitaeva, D.K.; Kalistratova, A.V.; Oshchepkov, M.S.; Kovalenko, L.V.; Kochetkov, K.A. Encapsulation of Chlorine-Containing Carbamates in Polypeptide Nanoparticles Prepared by Enzymatic Hydrolysis of Casein. *Russ. Chem. Bull.* **2018**, *67*, 1508–1512. [[CrossRef](#)]
11. Lee, E.H.; Chen, C.M. Studies on the Mechanisms of Ozone Tolerance: Cytokinin-like Activity of N-[2-(2-oxo-1-imidazolidinyl)Ethyl]-N'-phenylurea, a Compound Protecting against Ozone Injury. *Physiol. Plant.* **1982**, *56*, 486–491. [[CrossRef](#)]
12. Kannaujia, R.; Singh, P.; Prasad, V.; Pandey, V. Evaluating Impacts of Biogenic Silver Nanoparticles and Ethylenediurea on Wheat (*Triticum aestivum* L.) against Ozone-Induced Damages. *Environ. Res.* **2022**, *203*, 111857. [[CrossRef](#)]
13. Nigar, S.; Nazneen, S.; Khan, S.; Ali, N.; Sarwar, T. Response of *Vigna radiata* L. (Mung Bean) to Ozone Phytotoxicity Using Ethylenediurea and Magnesium Nitrate. *J. Plant Growth Regul.* **2021**, 1–13. [[CrossRef](#)]
14. Surabhi, S.; Gupta, S.K.; Pande, V.; Pandey, V. Individual and Combined Effects of Ethylenediurea (EDU) and Elevated Carbon Dioxide (CO<sub>2</sub>), on Two Rice (*Oryza sativa* L.) Cultivars under Ambient Ozone. *Environ. Adv.* **2020**, *2*, 100025. [[CrossRef](#)]
15. Motte, H.; Galuszka, P.; Spíchal, L.; Tarkowski, P.; Plíhal, O.; Šmehilová, M.; Jaworek, P.; Vereecke, D.; Werbrouck, S.; Geelen, D. Phenyl-Adenine, Identified in a LIGHT-DEPENDENT SHORT HYPOCOTYLS4-Assisted Chemical Screen, Is a Potent Compound for Shoot Regeneration through the Inhibition of CYTOKININ OXIDASE/DEHYDROGENASE Activity. *Plant Physiol.* **2013**, *161*, 1229–1241. [[CrossRef](#)]
16. Romanov, G.A.; Lomin, S.N.; Schmülling, T. Biochemical Characteristics and Ligand-Binding Properties of Arabidopsis Cytokinin Receptor AHK3 Compared to CRE1/AHK4 as Revealed by a Direct Binding Assay. *J. Exp. Bot.* **2006**, *57*, 4051–4058. [[CrossRef](#)]
17. Yonova, P. Design, Synthesis and Properties of Synthetic Cytokinins. Recent Advances on Their Application. *Gen. Appl. Plant Physiol.* **2010**, *36*, 124–147.
18. Weidner, C.; Rousseau, M.; Micikas, R.J.; Fischer, C.; Plauth, A.; Wowro, S.J.; Siems, K.; Hetterling, G.; Kliem, M.; Schroeder, F.C.; et al. Amorfrutin C Induces Apoptosis and Inhibits Proliferation in Colon Cancer Cells through Targeting Mitochondria. *J. Nat. Prod.* **2016**, *79*, 2–12. [[CrossRef](#)]
19. Kalistratova, A.V.; Kovalenko, L.V.; Oshchepkov, M.S.; Gamisoniya, A.M.; Gerasimova, T.S.; Demidov, Y.A.; Akimov, M.G. Synthesis of New Compounds in the Series of Aryl-Substituted Ureas with Cytotoxic and Antioxidant Activity. *Mendeleev Commun.* **2020**, *30*, 153–155. [[CrossRef](#)]
20. Searls, T.; McLaughlin, L.W. Synthesis of the Analogue Nucleoside 3-Deaza-2'-Deoxycytidine and Its Template Activity with DNA Polymerase. *Tetrahedron* **1999**, *55*, 11985–11996. [[CrossRef](#)]
21. Lougiakis, N.; Gavriil, E.-S.; Kairis, M.; Sioupouli, G.; Lambrinidis, G.; Benaki, D.; Kryptou, E.; Mikros, E.; Marakos, P.; Pouli, N.; et al. Design and Synthesis of Purine Analogues as Highly Specific Ligands for FcyB, a Ubiquitous Fungal Nucleobase Transporter. *Bioorg. Med. Chem.* **2016**, *24*, 5941–5952. [[CrossRef](#)]
22. Wang, Q.; Ye, B.; Wang, P.; Yao, F.; Zhang, C.; Yu, G. Overview of MicroRNA-199a Regulation in Cancer. *Cancer Manag. Res.* **2019**, *11*, 10327–10335. [[CrossRef](#)]
23. Voller, J.; Zatloukal, M.; Lenobel, R.; Doleal, K.; Bére, T.; Krytof, V.; Spíchal, L.; Niemann, P.; Dubák, P.; Hajdúch, M.; et al. Anticancer Activity of Natural Cytokinins: A Structure-Activity Relationship Study. *Phytochemistry* **2010**, *71*, 1350–1359. [[CrossRef](#)]
24. Cheng, R.K.Y.; Segala, E.; Robertson, N.; Deflorian, F.; Doré, A.S.; Errey, J.C.; Fiez-Vandal, C.; Marshall, F.H.; Cooke, R.M. Structures of Human A<sub>1</sub> and A<sub>2A</sub> Adenosine Receptors with Xanthines Reveal Determinants of Selectivity. *Structure* **2017**, *25*, 1275–1285.e4. [[CrossRef](#)]
25. Lebon, G.; Warne, T.; Edwards, P.C.; Bennett, K.; Langmead, C.J.; Leslie, A.G.W.; Tate, C.G. Agonist-Bound Adenosine A<sub>2A</sub> Receptor Structures Reveal Common Features of GPCR Activation. *Nature* **2011**, *474*, 521–525. [[CrossRef](#)] [[PubMed](#)]
26. Ozeir, M.; Huyet, J.; Burgevin, M.-C.; Pinson, B.; Chesney, F.; Remy, J.-M.; Siddiqi, A.R.; Lupoli, R.; Pinon, G.; Saint-Marc, C.; et al. Structural Basis for Substrate Selectivity and Nucleophilic Substitution Mechanisms in Human Adenine Phosphoribosyltransferase Catalyzed Reaction. *J. Biol. Chem.* **2019**, *294*, 11980–11991. [[CrossRef](#)] [[PubMed](#)]
27. Ludlow, R.F.; Verdonk, M.L.; Saini, H.K.; Tickle, I.J.; Jhoti, H. Detection of Secondary Binding Sites in Proteins Using Fragment Screening. *Proc. Natl. Acad. Sci. USA* **2015**, *112*, 15910–15915. [[CrossRef](#)] [[PubMed](#)]
28. Brown, N.R.; Lowe, E.D.; Petri, E.; Skamnaki, V.; Antrobus, R.; Johnson, L. Cyclin B and Cyclin A Confer Different Substrate Recognition Properties on CDK2. *Cell Cycle* **2007**, *6*, 1350–1359. [[CrossRef](#)] [[PubMed](#)]
29. Chen, J.-N.; Wu, D.-W.; Li, T.; Yang, K.-J.; Cheng, L.; Zhou, Z.-P.; Pu, S.-M.; Lin, W.-H. Arylurea Derivatives: A Class of Potential Cancer Targeting Agents. *Curr. Top. Med. Chem.* **2017**, *17*, 3099–3130. [[CrossRef](#)] [[PubMed](#)]
30. Naseem, M.; Othman, E.M.; Fathy, M.; Iqbal, J.; Howari, F.M.; AlRemeithi, F.A.; Kodandaraman, G.; Stopper, H.; Bencurova, E.; Vlachakis, D.; et al. Integrated Structural and Functional Analysis of the Protective Effects of Kinetin against Oxidative Stress in Mammalian Cellular Systems. *Sci. Rep.* **2020**, *10*, 13330. [[CrossRef](#)]
31. Spíchal, L.; Krystof, V.; Paprskářová, M.; Lenobel, R.; Styskala, J.; Binarová, P.; Cenklová, V.; De Veylder, L.; Inzé, D.; Kontopidis, G.; et al. Classical Anticytokinins Do Not Interact with Cytokinin Receptors but Inhibit Cyclin-Dependent Kinases. *J. Biol. Chem.* **2007**, *282*, 14356–14363. [[CrossRef](#)]
32. Gopinathan, L.; Tan, S.L.W.; Padmakumar, V.C.; Coppola, V.; Tessarollo, L.; Kaldis, P. Loss of Cdk2 and Cyclin A2 Impairs Cell Proliferation and Tumorigenesis. *Cancer Res.* **2014**, *74*, 3870–3879. [[CrossRef](#)]
33. Gessi, S.; Bencivenni, S.; Battistello, E.; Vincenzi, F.; Colotta, V.; Catarzi, D.; Varano, F.; Merighi, S.; Borea, P.A.; Varani, K. Inhibition of A<sub>2A</sub> Adenosine Receptor Signaling in Cancer Cells Proliferation by the Novel Antagonist TP455. *Front. Pharmacol.* **2017**, *8*, 888. [[CrossRef](#)]

34. Takahashi, S.; Shudo, K.; Okamoto, T.; Yamada, K.; Isogai, Y. Cytokinin Activity of N-Phenyl-N'-(4-Pyridyl)Urea Derivatives. *Phytochemistry* **1978**, *17*, 1201–1207. [[CrossRef](#)]
35. Baskakov, J.A.; Shevelukha, V.S.; Simonov, V.D.; Kulaeva, O.N.; Chimishkian, A.L.; Butenko, R.G.; Shapovalov, A.A.; Nedelchenko, B.M.; Shanbanovich, G.N.; Taschi, V.P.; et al. Carbamoyl Derivatives of Alkanolamines and Antistress-Type Means for Plant Growth Regulation Based Thereon. WO1991007381A1, 30 May 1991.
36. van de Loosdrecht, A.A.; Beelen, R.H.J.; Ossenkoppele, G.J.; Broekhoven, M.G.; Langenhuijsen, M.M.A.C. A Tetrazolium-Based Colorimetric MTT Assay to Quantitate Human Monocyte Mediated Cytotoxicity against Leukemic Cells from Cell Lines and Patients with Acute Myeloid Leukemia. *J. Immunol. Methods* **1994**, *174*, 311–320. [[CrossRef](#)]
37. O'Boyle, N.M.; Banck, M.; James, C.A.; Morley, C.; Vandermeersch, T.; Hutchison, G.R. Open Babel: An Open Chemical Toolbox. *J. Cheminform.* **2011**, *3*, 33. [[CrossRef](#)]
38. Ramachandran, S.; Kota, P.; Ding, F.; Dokholyan, N.V. Automated Minimization of Steric Clashes in Protein Structures. *Proteins* **2011**, *79*, 261–270. [[CrossRef](#)]
39. Trott, O.; Olson, A.J. AutoDock Vina: Improving the Speed and Accuracy of Docking with a New Scoring Function, Efficient Optimization, and Multithreading. *J. Comput. Chem.* **2010**, *31*, 455–461. [[CrossRef](#)]
40. Maslova, V.D.; Reshetnikov, R.V.; Bezuglov, V.V.; Lyubimov, I.I.; Golovin, A.V. Supercomputer Simulations of Dopamine-Derived Ligands Complexed with Cyclooxygenases. *Supercomput. Front. Innov.* **2018**, *5*, 98–102. [[CrossRef](#)]
41. Ankerst, M.; Breunig, M.M.; Kriegel, H.-P.; Sander, J. OPTICS: Ordering Points to Identify the Clustering Structure. *SIGMOD Rec.* **1999**, *28*, 49–60. [[CrossRef](#)]
42. Pedregosa, F.; Varoquaux, G.; Gramfort, A.; Michel, V.; Thirion, B.; Grisel, O.; Blondel, M.; Prettenhofer, P.; Weiss, R.; Dubourg, V.; et al. Scikit-Learn: Machine Learning in Python. *J. Mach. Learn. Res.* **2011**, *12*, 2825–2830.